THE WORLD OF TWO QUBITS

Gili Bisker

THE WORLD OF TWO QUBITS

Research Thesis

Submitted in partial fulfillment of the requirements for the degree of
Master of Science in Physics

Gili Bisker

Submitted to the Senate of the Technion - Israel Institute of Technology
Kislev 5768 HAIFA December 2007

This research thesis was done under the supervision of
Prof. Joseph E. Avron in the Department of Physics

I would like to express my deepest sense of gratitude to my supervisor, prof. Joseph E. Avron, for invaluable guidance and constant support. His encouragement and excellent advice have made this thesis possible.

I am thankful to Dr. Oded Kenneth for his generous assistance and for his patient way of sharing his experience and knowledge.

Finally, I would like to thank my beloved family and friends for their moral support and for being the driving force in my life.

The generous financial support of
The Technion
is gratefully acknowledged.

Contents

List of Figures

List of Tables

Abstract

The world of states, witnesses and Bell inequalities of two qubits can be visualized geometrically. Since it is represented by 4×4 Hermitian matrices, it is 16 dimensional. Thus, visualization in three dimensions requires introducing an appropriate equivalence relation. The SLOCC equivalence relation is often used for states and here we show that entanglement witnesses and CHSH Bell inequalities can be incorporated in this description as well.

The geometric description is faithful to the duality between separable states and witnesses, and allows one to give elementary and elegant proofs of non-elementary results.

This visualization allows us to give a "proof by inspection" that for two qubits, the Peres test is 'if and only if'. We show that the CHSH Bell inequalities, where both Alice and Bob have two experiments to choose from, can be visualized as circles in the figure. This allows us to solve geometrically the optimization problem of the CHSH inequality violation. Finally, we give numerical evidence that, remarkably, allowing Alice and Bob to use three rather than two measurements, does not help them to distinguish any new entangled SLOCC equivalence class beyond the CHSH class.

The concept of entanglement witnesses has a practical meaning as well. If one wants to prove the existence of entanglement, two approaches can be used. The first one is to find the state explicitly and use the Peres separability test mentioned above. The second is to measure the expectation value of a corresponding entanglement witness. The latter is more economical, since the number of measurements needed is smaller, whereas in the first approach no less then 16 measurements are needed. We present a set of product projective measurements, optimal for proving entanglement. Our goal is to minimize the number of measurements needed in order to find the expectation value of an entanglement witness.

List of Symbols

symbol	**Meaning**
ρ	Density matrix
ρ^{pt}	Partial transposition of a density matrix
σ^j	Pauli matrix
η	Minkowski metric tensor $diag(1,-1,-1,-1)$
LHV	Local hidden variable
LOCC	Local operation and classical communication
SLOCC	Stochastic local operation and classical communication
$SL(2,\mathbb{C})$	2×2 complex matrices with determinant 1
$SU(2)$	2×2 unitary matrices with determinant 1
F^K	Farkas vector
Z^K	Trivial Farkas vector
$\{\rho\}$	The set of states
$\{\rho_s\}$	The set of separable states
$\{W_e\}$	The set of potential entanglement witnesses
$\{\rho\}_B$	The set of states satisfying a Bell inequality
$\{\rho\}_B^{SLOCC}$	The set of states satisfying a Bell inequality in a SLOCC sense

1 Introduction

The field of Quantum Information has been rapidly developing during the past couple of decades [1]. The special features of quantum mechanics are exploited for new algorithms [2] that are possible only in the quantum regime. Since the famous EPR paper [3] a lot of effort has been put into understanding the full potential of entanglement [4] of two qubits. The Bell states, which are maximally entangled states of two qubits, are of extreme value in quantum information. For instance, a Bell state is required for "Teleportation" [5], which is one of the most important quantum algorithms.

Deciding whether a state of two qubits is entangled or not can be tricky. Peres [6] gave a simple necessary condition for a state to be separable and it is reviewed is section 1.1. This condition was proven to be sufficient by the Horodeckis [7], who used the concept of "Entanglement Witnesses". Every entangled state has a corresponding witness that identifies it as entangled [7]:

Theorem 1.1. *A state ρ is entangled if and only if there exists an observable W, such that $Tr(W\sigma) \geq 0$ for all separable states σ, and $Tr(W\rho) < 0$. The operator W is called an entanglement witness.*

Another test for entanglement, which is only sufficient but not necessary, is Bell inequality [8]. If a state violates one, it is necessarily entangled, but the opposite claim is false. The simplest Bell inequality in the case of two observers is CHSH inequality [9], where both Alice and Bob have two dichotomic experiments to choose from. The statistics of their mutual results must satisfy the CHSH inequality in the framework of local hidden variable theory (LHV). Thus, all the separable states satisfy all the Bell inequalities [10].

In section 1.2 we give a procedure of finding all the Bell inequalities [11]. Asher Peres described in [11] how to construct all the Bell inequalities for any number of observers, each having any number of measurements to choose from, where each measurement has any number of possible outcomes. We briefly review the main results and use them for the CHSH [9] case, where we construct the corresponding Farkas vector. In addition, we give a Farkas vector corresponding to a more general case, where both Alice and Bob have three dichotomic experiments to choose from.

The visualization of the world of two qubits [12] is described in chapter 2. We start with 16 dimensions and rely on notions of equivalence in order to reduce the number of dimensions from 16 to 3. An effective notion of equivalence is SLOCC [13, 14]. It is often used for states, but here, we broaden the notion of equivalence to entanglement witnesses. Doing so, we can visualize Bell inequalities in 3 dimensions as well.

The measurement of the entanglement witness is explain in chapter 3. We develop a tool that can effectively tell, using as few measurements as possible, if a quantum state is entangled or not, without having to reconstruct the entire density matrix. We use the fact that finding an expectation value of an entanglement witness requires less measurements than reconstructing the quantum state completely. We give an example of an entangled quantum state of two qubits, its corresponding witness, and the minimal set of local measurements needed in order to prove it is indeed entangled.

1.1 The Peres Test for Separability

A quantum system of two qubits can be either entangled or separable. If the state of the system is pure, $|\psi\rangle$, then it is separable if it can be written as a product of two one qubit states:

$$|\psi\rangle = |\phi^a\rangle \otimes |\phi^b\rangle \tag{1.1}$$

In that case, finding the Schmidt number of the state is a straightforward way to check whether a pure state is entangled or not.

Generically, the state of two qubits is mixed, and identifying entanglement seems to be more difficult a priori. A separable state of two qubits can be written in the form [6]:

$$\rho = \sum_i w_i \rho_i^A \otimes \rho_i^B \tag{1.2}$$

where $w_i \geq 0$ and $\sum_i w_i = 1$.

Let us define the operation of partial transposition on a general 4×4 matrix. In order to partially transpose a 4×4 matrix, one has to transpose the four 2×2 blocks:

$$\begin{pmatrix} a_1 & a_2 & b_1 & b_2 \\ a_3 & a_4 & b_3 & b_4 \\ c_1 & c_2 & d_1 & d_2 \\ c_3 & c_4 & d_3 & d_4 \end{pmatrix}^{pt} = \begin{pmatrix} a_1 & a_3 & b_1 & b_3 \\ a_2 & a_4 & b_2 & b_4 \\ c_1 & c_3 & d_1 & d_3 \\ c_2 & c_4 & d_2 & d_4 \end{pmatrix} \tag{1.3}$$

In this case of a separable density matrix (1.2), the partial transposed matrix:

$$\rho^{pt} = \sum_i w_i \rho_i^A \otimes \left(\rho_i^B\right)^T \tag{1.4}$$

is also a legitimate density matrix, since $(\rho^B)^T = (\rho^B)^*$ is a legitimate one qubit state if ρ^B is. This gives a necessary condition for a density matrix to be separable [6]: if the

partial transposed matrix is not a state, meaning, one of its eigenvalues is negative, than the original state cannot be separable. The sufficiency of the Peres test was first proven by the Horodeckis [7] for systems of two qubits and for systems of a qubit and a qutrit (dimension 2×3) as well.

1.2 Bell Inequalities

Bell's Theorem [8] says that one can never formulate a full description of the predictions of quantum mechanics by local hidden variables (LHV) theory. Bell's inequality should hold in the framework of such a theory, so if a state violates such an inequality, one cannot describe it using LHV theory.

1.2.1 Constructing all the Bell Inequalities

A general Bell inequality can be written as [11]

$$\sum_K F^K P_K \geq 0 \tag{1.1}$$

where $\{P_K\}$ are the outcomes' probabilities, that can be measured experimentally, and $\{F^K\}$ are integer coefficients. The indices $\{K\}$ run on all the possible measurements' outcomes. Here we construct a way to find the coefficients $\{F^K\}$ in the following case: There are two observers, Alice and Bob, both having $N_A = 2$ and $N_B = 2$ experiments to choose from, respectively, and their jth experiment has $A_j = 2$ and $B_j = 2$ possible outcomes, respectively. This setup is illustrated in figure 1.

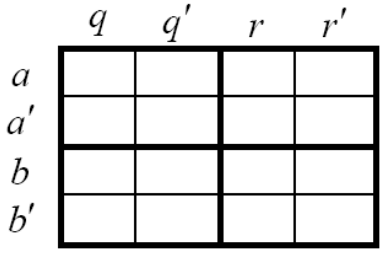

Figure 1: System setup of a Bell inequality: Alice has two experiments to choose from (A and B), Bob also has two measurements to choose from (Q and R). Each measurement X has two possible outcomes x and x'.

A hidden variable λ describes the outcome of every possible combination of two measurements chosen by Alice and Bob. For example, if $\lambda = [ab; q'r']$ then if Alice chose

experiment A and Bob chose experiment R, the measurements' outcome K is $K = ar'$, see figure 2.

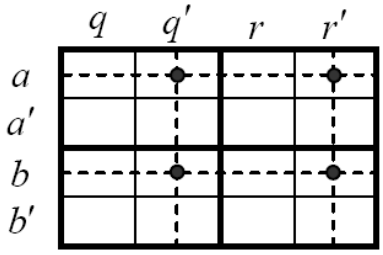

Figure 2: The hidden variable $\lambda = [ab; q'r']$.

The number of possible outcomes is $N_k = (\sum_i A_i)(\sum_j B_j) = 16$, which is exactly the number of lattice points in figure 2. The number of hidden variables is $N_\lambda = (\prod_i A_i)(\prod_j B_j) = 16$, which is exactly the number of different ways to build nets as in figure 2. Since both Alice and Bob can choose one of N_A and N_B possible experiments respectively, together they have $N_c = N_A N_B = 4$ possible pairs of experiments.

We define a boolean matrix B_K^λ of size $N_k \times N_\lambda$ in the following way:

$$B_K^\lambda = \begin{cases} 1 & \text{The outcome } K \text{ is possible for the hidden varible } \lambda \\ 0 & \text{otherwise} \end{cases} \tag{1.2}$$

For example:

$$B_{ar'}^{[ab;q'r']} = (\delta_a^a + \delta_a^b)(\delta_{r'}^{q'} + \delta_{r'}^{r'}) = 1 \tag{1.3}$$

but

$$B_{ar}^{[ab;q'r']} = (\delta_a^a + \delta_a^b)(\delta_r^{q'} + \delta_r^{r'}) = 0 \tag{1.4}$$

For each hidden variable λ, $\sum_K B_K^\lambda = N_c$. We define vectors $\mathbf{B}^\lambda$ whose components are B_K^λ. These vectors are not linearly independent, for example:

$$B^{[ab;q'r']} + B^{[ab;qr]} = B^{[ab;qr']} + B^{[ab;q'r]} \tag{1.5}$$

In addition, none of the vectors $\mathbf{B}^\lambda$ can be expressed as a convex combination of the others, so each vector $\mathbf{B}^\lambda$ can be considered as an extreme ray of a convex cone. The matrix B_K^λ can be described figuratively for each λ by placing 0 or 1 in the lattice of figure 2, see figure 3.

If denote by w_λ the probability of the hidden variable λ then the probability of the outcome K is:

$$P_K = \sum_\lambda P(\lambda)P(K|\lambda) = \sum_\lambda w_\lambda B_K^\lambda \tag{1.6}$$

	q	q'	r	r'
a	0	1	0	1
a'	0	0	0	0
b	0	1	0	1
b'	0	0	0	0

Figure 3: The entries of the boolean matrix B_K^λ for $\lambda = [ab; q'r']$.

The vector $\mathbf{P}$ with components P_K is a convex combination of the boolean vectors $\mathbf{B}^\lambda$, which is a necessary and sufficient condition for the existence of the hidden variables λ. In order to determine whether a vector $\mathbf{P}$ lies inside the convex cone defined by the vectors $\mathbf{B}^\lambda$, one can use Farkas' lemma [15, 16]. The Farkas lemma in our case is:

$$\left(\exists w_\lambda \geq 0\,,\ \sum_\lambda w_\lambda B_K^\lambda = P_K\right) \Longleftrightarrow \left(\forall F^K \left\{\sum_K B_K^\lambda F^K \geq 0 \Rightarrow \sum_K P_K F^K \geq 0\right\}\right) \quad (1.7)$$

If a local hidden variable theory that is consistent with the probabilities of the measurements' outcomes $\{P_K\}$ exists, meaning, there are $w_\lambda \geq 0$ such that

$$P_K = \sum_\lambda w_\lambda B_K^\lambda \quad (1.8)$$

then for every vector F^K such that

$$\sum_K B_K^\lambda F^K \geq 0 \quad (1.9)$$

then

$$\sum_K P_K F^K \geq 0 \quad (1.10)$$

Equation (1.10) is a Bell inequality, and the vector F^K is a Farkas vector. The Farkas vectors can also be described figuratively as the matrix B_K^λ in figure 3.

Now we need to construct as many Farkas vectors as possible. A Farkas vector with positive entries is not interesting, since the probabilities $\{P_K\}$ are positive equation (1.10) holds trivially. Thus, we are interested in Farkas vectors with some negative entries. Trivial Farkas vectors are described in figure 4. We denote them as Z^K, and they have the property that for every hidden variable λ, $\sum_K B_K^\lambda Z^K = 0$.

There are 7 independent trivial Farkas vectors in our case, see figure 5.

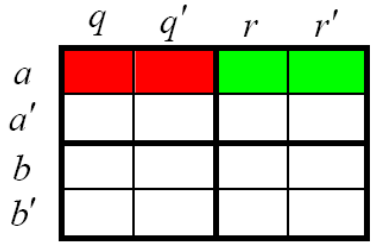

Figure 4: Trivial Farkas vectors Z^K. The red cells represent the value -1, the green cells represent $+1$ and the white cells represent 0. The value of $\sum_K B_K^\lambda Z^K$ is calculated by looking at this figure of the Farkas vector Z^K and figure 3 of the matrix B_K^λ. One can convince oneself that for every λ, $\sum_K B_K^\lambda Z^K = 0$. This equality holds for the outcomes' probabilities as well, $\sum_K P_K Z^K = 0$. For the vector given here, the latter means that the probability that Alice got the outcome a is independent of which measurement Bob chooses to perform.

If F^K is a Farkas vector, and Z^K is a trivial one, then for every real x, $G^K = F^K + xZ^K$ is a Farkas vector as well. We can therefore define equivalence classes of Farkas vectors using this relation.

The procedure of finding a relevant Farkas vector is illustrated in figure 6. In our case there are 64 Farkas vectors that are divided into 8 equivalence classes, see figure 7.

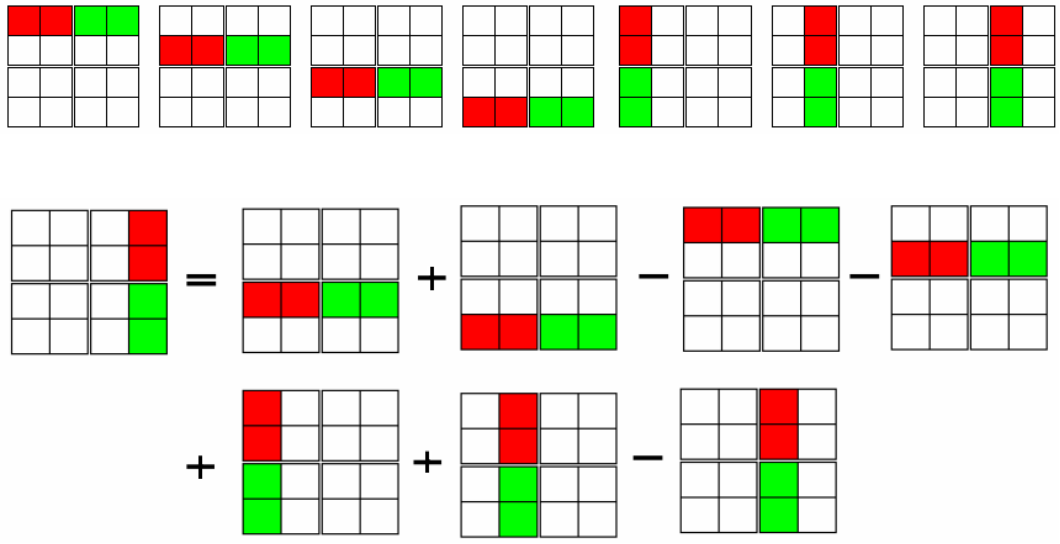

Figure 5: Top: The 7 trivial Farkas vectors in our case. Bottom: the 8th trivial Farkas vector is a linear combination of the first 7.

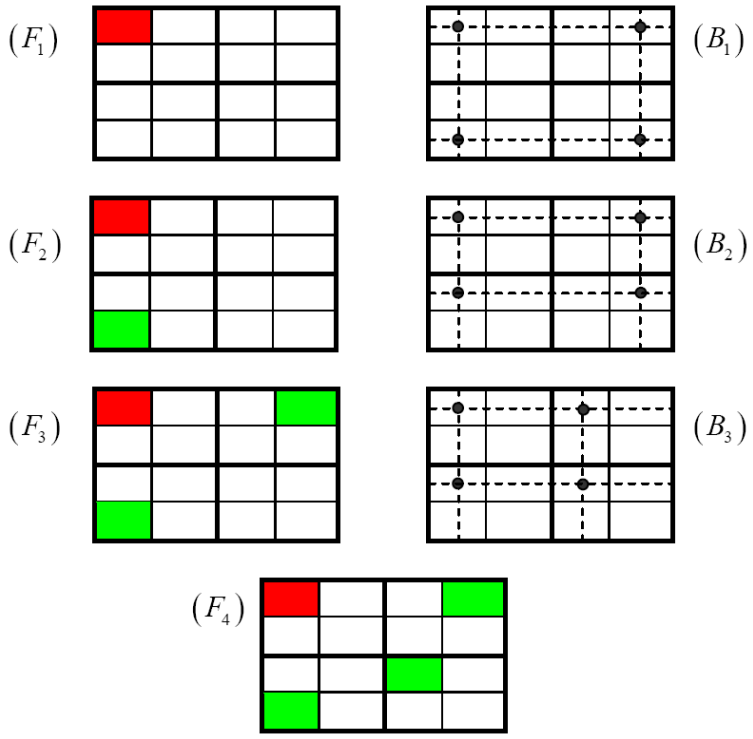

Figure 6: Constructing a Farkas vector. We start with one negative entry (F_1). We need the inequality (1.9) to hold, but (B_1) is an example of a matrix B_K^λ for which the desired inequality does not hold. Adding a positive entry to the Farkas vector (F_2) is not enough, due to (B_2). Another positive entry (F_3) is still not enough, since (B_3) violates the inequality. Finally, (F_4) is a legitimate Farkas vector, for which the inequality (1.9) holds for all B_K^λ.

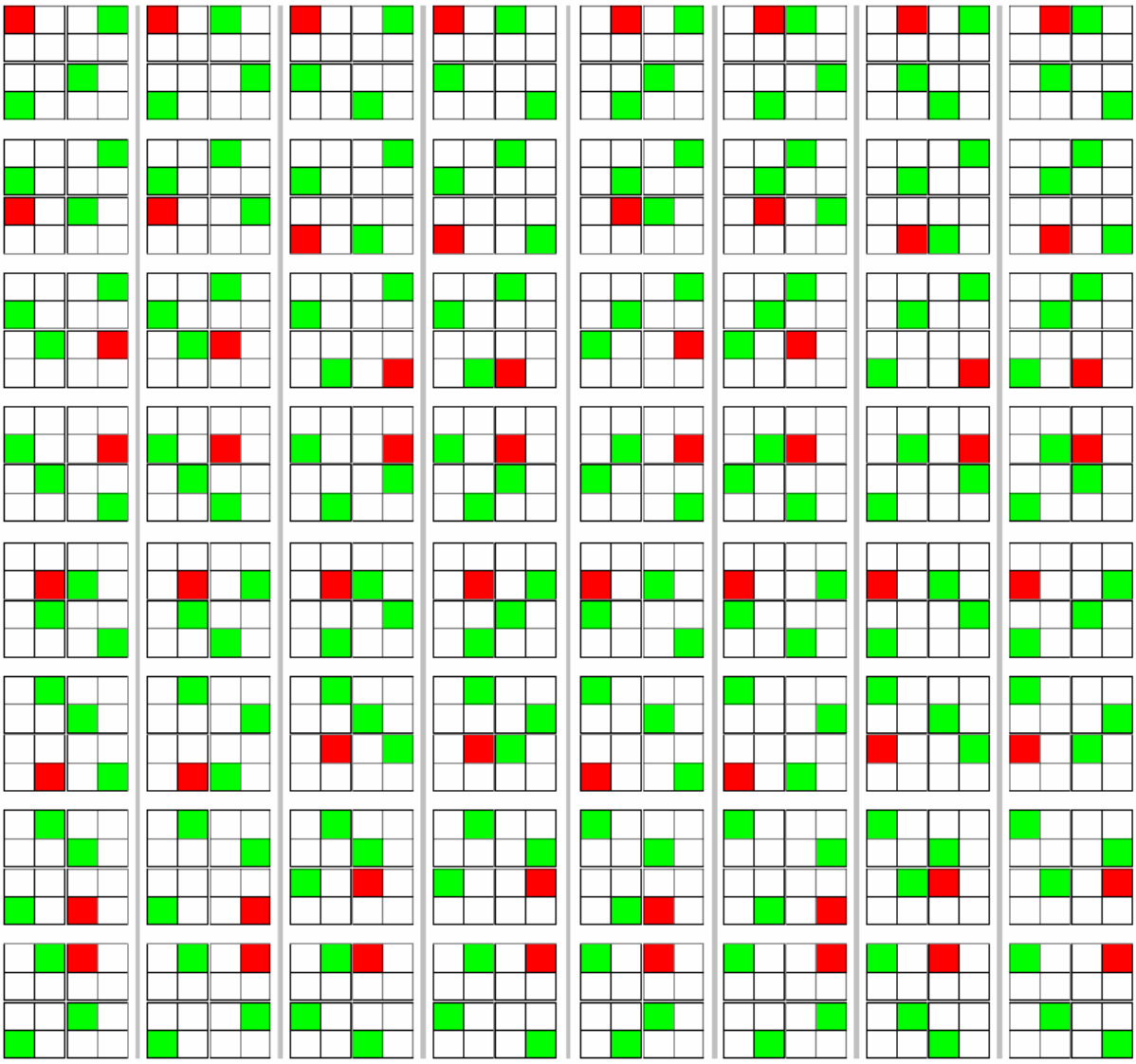

Figure 7: All the 64 Farkas vectors in 8 equivalence classes.

1.2.2 Farkas Vector of CHSH Inequality

Let us choose the Farkas vector that was constructed in figure 6:

$$F^K = \begin{cases} -1 & K = aq \\ 1 & K \in \{ar', br, b'q\} \\ 0 & \text{otherwise} \end{cases} \tag{1.11}$$

The Bell inequality (1.10) is written in the form:

$$P_{ar'} + P_{br} + P_{b'q} - P_{aq} \geq 0 \tag{1.12}$$

By adding and subtracting $P_{bq} + P_{ar}$, we have

$$P_a + P_q + P_{br} - P_{aq} - P_{bq} - P_{ar} \geq 0 \tag{1.13}$$

Substituting P_{xy} by $\frac{1}{2}(I + \vec{x} \cdot \vec{\sigma}) \otimes \frac{1}{2}(I + \vec{y} \cdot \vec{\sigma})$ we find the CHSH inequality [9]:

$$\left(\vec{a} \cdot \vec{\sigma} \otimes (\vec{r} + \vec{q}) \cdot \vec{\sigma} - \vec{b} \cdot \vec{\sigma} \otimes (\vec{r} - \vec{q}) \cdot \vec{\sigma}\right) \leq 2 \tag{1.14}$$

The inequalities corresponding to different equivalence classes of Farkas vectors are CHSH inequalities as well, and they are obtained by swapping one or more outcomes $x \leftrightarrow x'$ in equation (1.14).

In [17], Collins and Gisin looked for all the Bell inequalities for the setting described here, two observers, each with two dichotomic measurements to choose from. They found numerically that the CHSH inequality is the only relevant Bell inequality in this case. They found 8 versions of CHSH inequality corresponding to the 8 equivalence classes of Farkas vectors. The fact that the CHSH inequality is the only relevant one in the given setting was also proven analytically in [18]. With the description of Farkas vectors, we gain very good intuition of this idea. In fact, one can convince oneself that no other Farkas vectors can be found.

1.2.3 Farkas Vector of a more general Bell Inequality

Gisin and Collins [17] gave an explicit form of a Bell inequality, where both Alice and Bob have three dichotomic experiments to choose from. This inequality is denoted as I_{3322} and is discussed in section 2.5.

The relevant Farkas vector for I_{3322} is given in figure 8 and the inequality that it describes is:

$$P_{aq'} - 2P_{ar} - P_{ar'} + P_{as'} + P_{b'q} + P_{b'r} + P_{bs} + P_{c'q} + P_{cr} \geq 0 \tag{1.15}$$

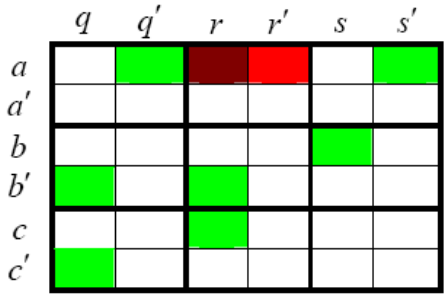

Figure 8: Farkas vector for I_{3322}. The dark red color stands for -2.

The inequality can be written using different notations. The experiments have two possible outcomes, say the outcome x stands for 0 and x' stands for 1. We denote by $P(A_iB_j)$ the probability that both Alice and Bob got the outcome 0, when Alice chooses the ith measurement and Bob chooses the jth measurement. Renaming Alice's experiments A_1, A_2, A_3 and Bob's experiments B_1, B_2, B_3 respectively, we can substitute, for example, P_{ar} by $P(A_1B_2)$ and $P_{aq'}$ by $P(A_1) - P(A_1, B_1)$. The inequality with these notations is given in equation (2.37).

2 Visualizing Two Qubits and Bell Inequalities

2.1 Introduction

Any 4×4 hermitian operator W can be represented by a 4×4 real matrix ω as follows:

$$W = \omega_{\mu\nu} \sigma^\mu \otimes \sigma^\nu \tag{2.1}$$

Greek indices run on $0, 1, 2, 3$, Roman indices on $1, 2, 3$. σ^0 is the identity and σ^j are the Pauli matrices. Summation over a pair of repeated indices is always implied, and indices are raised and lowered using the Minkowski metric tensor $\eta = diag(1, -1, -1, -1)$. To reduce the number of components from 16 to 3 one relies on notions of equivalence. In particular, forgetting about the overall normalization of operators reduces the dimension by 1.

An effective notion of equivalence comes from allowing Alice and Bob to operate on their respective qubits

$$\rho \to \rho^M = M \, \rho \, M^\dagger, \quad M = A \otimes B, \tag{2.2}$$

We shall focus on the case $A, B \in SL(2, \mathbb{C})$ where the operation is invertible but not trace preserving. The physical interpretation of this is that states which are accessible by local, reversible filtering are identified. It is known as SLOCC [13, 14] and is briefly reviewed in section 2.2. Since $\dim SL(2, \mathbb{C}) = 6$ the SLOCC equivalence reduces the dimension by 12. As a consequence, the SLOCC equivalence classes of unnormalized 2 qubits states can be visualized in 3 dimensions.

As we shall see, the SLOCC equivalence classes of entanglement witnesses are represented by the cube, the states by the tetrahedron and the separable states by the octahedron of Fig. 9. The octahedron and tetrahedron have been identified as the SLOCC representation in [19, 20]. Adding the cube as a representation of the SLOCC equivalence classes of entanglement witnesses shows that the natural duality relation between witnesses and separable states is preserved in the visualization of the SLOCC equivalence classes: The cube is the dual of the octahedron in the usual sense of duality of convex sets [21]. In particular, the number of faces in one is the number of vertices in the other. The tetrahedron is, of course, its own dual.

Since the work of the Horodeckis, [22], Fig. 9 has been widely used in quantum information theory for the special cases of states with maximally mixed subsystems [23, 24]. This is a 9 dimensional family of states with $\omega_{0j} = \omega_{j0} = 0$ in Eq. (2.1). Since this family has a lower dimension, it can be visualized in 3 dimensions using a more restrictive notion

of equivalence than SLOCC: Alice and Bob are allowed to perform only unitary operations on their respective qubits with $A, B \in SU(2)$ in Eq. (2.2). This in arguably the most fundamental notion of equivalence in quantum information theory and is known as LOCC [1, 4]. It is trace preserving, which expresses the fact that, unlike SLOCC, it is not lossy, (no state is ever discarded). Since $\dim SU(2) \times SU(2) = 6$ the LOCC equivalence classes of this 9 dimensional family of states can be represented in 3 dimensions [22]. It is remarkable that both the visualization and the interpretation of Fig. 9 remain the same when one goes from the 9 dimensional family to the 16 dimensional family of general 2 qubits states. All that changes is the notion of equivalence.

Fig. 9 turns out to play a significant role also in the theory of quantum communication. Namely, it characterizes the stochastic properties of certain *single qubit* quantum channels as shown in [25, 26, 27]. This rather different interpretation of the figure follows from a deep relation, known as the Choi-Jamiolkwosky isomorphism [28], between linear operators acting on the Hilbert space of Alice and Bob, and linear maps on single qubit states. Using this, one finds [25, 26, 27] that (for unital[1] and trace preserving channels) the octahedron represents channels that destroy entanglement, the tetrahedron represents the completely positive maps and the cube represents the positive maps.

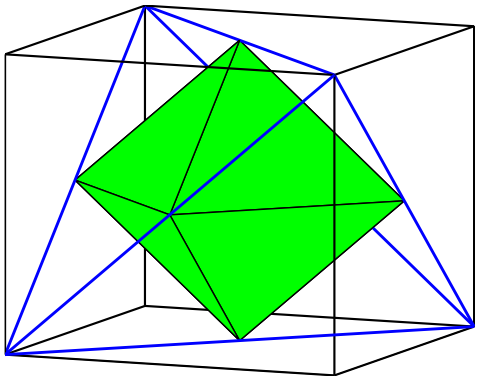

Figure 9: Three dimensional view of the world of two qubits: The cube represents the equivalence classes of potential entanglement witnesses, the tetrahedron represents the states, and the octahedron represents the separable states.

In section 2.3 we shall review the SLOCC interpretation of Fig. 9 from a perspective that focuses on the duality relations between the sets in the figure. The main new re-

[1] A unital map is one that maps the unit operator to itself.

sults concern the visualization of entanglement witnesses, duality and of the CHSH Bell inequalities.

2.2 Local operations

The local mapping of a two qubit state ρ given by Eq. (2.2) preserves positivity and takes a product state $\rho_A \otimes \rho_B$ to a product state. It therefore maps any separable state—a convex combination of product states—to a separable state. This makes the equivalence $\rho \sim \rho^M$, a useful notion in studying the entanglement of two qubits [19, 20]. Since the operation does not preserve the normalization of the state, it is convenient to consider states up to normalization. The operations performed by Alice and Bob can be interpreted as *probabilistically reversible filtering* associated with the POVMs

$$E_1^{(M)} = \frac{M^\dagger M}{||M||^2}, \quad E_2^{(M)} = 1 - E_1^{(M)}$$

($E_2^{(M)}$ is not a local operator; local POVM would require 4 E_i's). The probability of successfully filtering the state $\rho^M/Tr(\rho^M)$ is strictly positive and is given by $Tr(\rho E_1^{(M)}) > 0$. (If M is unitary the filtering succeeds with probability one). It is probabilistically reversible since the original state ρ can be recovered, with non-zero probability, from ρ^M using the filter $E_1^{(M^{-1})}$.

One can broaden the notion of equivalence under SLOCC from states to observables and in particular, to witnesses W. We take the action on witnesses to be contragradient to that of states:

$$W \to W^M = (M^\dagger)^{-1}\, W\, M^{-1}, \quad M = A \otimes B, \quad A, B \in SL(2, \mathbb{C}) \tag{2.3}$$

(If M is unitary, states and observables transform the same way). The motivation for this choice is to have ρW transform by a similarity transformation so its trace, and therefore the associated expectation and probability, is left invariant.

2.2.1 Potential witnesses

We shall say that W_e is a *potential entanglement witness* if[2]

$$Tr(W_e \rho_s) \geq 0 \tag{2.4}$$

[2]For a definition of witnesses that goes through the Choi-Jamiolkowsky isomorphism, see e.g. [29].

for all separable states ρ_s. Since the set of separable states $\{\rho_s\}$ is a convex cone in the space of 4×4 matrices, the set of potential entanglement witnesses $\{W_e\}$ is the dual convex cone of $\{\rho_s\}$. The set of states, $\{\rho\}$, is a convex cone as well, and the three convex cones are evidently nested

$$\{\rho_s\} \subset \{\rho\} \subset \{W_e\} \tag{2.5}$$

The cones $\{\rho\}$, $\{\rho_s\}$ and $\{W_e\}$ all lie in 16 dimensions, which is not very useful for visualization.

SLOCC takes a potential entanglement witness to a potential entanglement witness. This follows from

$$Tr(W_e^M \rho_s) = Tr(W_e \rho_s^{M^{-1}}) \geq 0 \tag{2.6}$$

which shows that W_e^M is an entanglement witness if W_e is.

SLOCC allows one to reduce the study of states, separable states, and (potential) entanglement witnesses to the study of the corresponding equivalence classes. As will be explained in section 2.3, the equivalence classes of the three cones are described by the three polyhedra shown in Fig. 9.

Similar ideas can be used to visualize Bell inequalities, as we now proceed to show.

2.2.2 Bell witnesses

Every Bell inequality has a corresponding witness [30]. Let W_B be a witness for a specific Bell inequality. A state ρ_h satisfies this Bell inequality if

$$Tr(W_B \rho_h) \geq 0 \tag{2.7}$$

Since the separable states satisfy all types of Bell inequalities [30, 4], it is clear that W_B belongs to the family of potential entanglement witness. The set $\{\rho\}_B$ of states satisfying (2.7) for a specific type of Bell inequalities (e.g. the CHSH family) forms a convex cone. However, in general it is larger than the cone $\{\rho_s\}$ of separable states.

2.2.3 CHSH witnesses

The CHSH Bell inequalities describe a situation where Alice may choose to measure her qubits in one of two directions, (a, a') and Bob may similarly choose one of the directions, (b, b'). It is represented by the witness [30]

$$W_B = \frac{1}{2}\left(2 \pm B_{CHSH}\right) \tag{2.8}$$

where B_{CHSH} is the CHSH operator [9]:

$$B_{CHSH}(a, a', b, b') = a \cdot \sigma \otimes (b + b') \cdot \sigma + a' \cdot \sigma \otimes (b - b') \cdot \sigma \tag{2.9}$$

$a \cdot \sigma = a_j \sigma^j$. The CHSH Bell inequality then takes the form of Eq. (2.7).

The family of all CHSH witnesses is an a-priori 8 dimensional family associated with the 4 directions Alice and Bob choose. (In fact, an implicit degeneracy in Eq. (2.9) makes it only 7 dimensional.) LOCC takes a CHSH witness corresponding to the directions (a, a', b, b') to a witness associated with rotated directions while keeping $a \cdot a'$ and $b \cdot b'$ fixed. This reduces the dimension by 6 and allows us to visualize the equivalence classes of CHSH witnesses. As we explain in section 2.4, they turn out to be the three circles shown in Fig. 11 on page 25.

2.2.4 Bell inequalities and SLOCC

Local operations (Eq. (2.2)) are guaranteed to take separable states to separable states. This reflects the fact that no entangled state can ever be (locally) filtered from a separable state. This is not the case for states that satisfy Bell inequalities. In fact, [31] gave examples of states satisfying all the CHSH inequalities whose filtration violate the inequality. This is consistent because the positivity of $Tr(W_B \rho_h)$ *does not* imply positivity of $Tr(W_B \rho_h^M)$. SLOCC does not act nicely on CHSH. This can also be seen from the fact that the family of CHSH witnesses *is not* mapped on itself by SLOCC. It is therefore *not possible* to represent the states that satisfy CHSH inequalities in terms of their SLOCC equivalence classes.

It seems clear, however, that if a state ρ^M, filtered from ρ (using only local operations), breaks a certain Bell inequality then the properties of ρ itself are inconsistent with (more general) local hidden variables. Indeed, if ρ would have been describable in terms of hidden variables, that would have implied that the results of any experiment done on it including one involving local filtration (which is also a type of measurement) should be explainable in terms of these hidden variables[3].

This motivates the introduction of a notion of states that satisfy Bell inequality in a SLOCC sense by requiring that not only the state ρ_h satisfy the Bell inequality W_B (2.7),

[3]It turns out that the combined experiment done on ρ consisting of filtration plus subsequent spin measurement can be described using hidden variables, only if the choice of Alice whether to measure a or a' can influence the result of the filtration which was completed prior to it. This breaks natural causality assumptions. The fact that ρ does not itself break Bell's inequality may then be traced to the fact that the standard derivation of Bell's inequalities does not involve these causality assumptions.

but also that all states that can be *probabilistically filtered* from ρ_h do. This is clearly a SLOCC invariant notion. Mathematically, it is expressed by the requirement

$$\inf_M Tr(W_B \rho_h^M) \geq 0 \tag{2.10}$$

We shall denote this set $\{\rho\}_B^{SLOCC}$. It is, of course, a smaller set, $\{\rho\}_B^{SLOCC} \subset \{\rho\}_B$, but it is not empty. This set is SLOCC invariant and so may be visualized in three dimensions. The corresponding 3-dimensional set is the intersection of 3 cylinders shown in Fig. 12 on page 26, as we shall explain in section 2.4. For any fixed witness W_B the equivalence class $\{\rho\}_B^{SLOCC}$ is a convex cone since

$$\inf_M Tr(W_B(\rho_1+\rho_2)^M) \geq \inf_M Tr(W_B\rho_1^M) + \inf_M Tr(W_B\rho_2^M) \tag{2.11}$$

Since the intersection of convex cones is a convex cone, it follows that the states that satisfy *a family* of Bell inequalities in the SLOCC sense also form a convex cone. In particular, this is so for the CHSH family. The intersection of the cone with the hyperplane $Tr\rho = 1$ is then evidently a convex set.

Similarly, the dual (convex) cone to $\{\rho\}_B^{SLOCC}$ is SLOCC invariant by Eq. (2.6), i.e. if W_B is a witness for a given SLOCC family, so is W_B^M. These notions of witnesses and states conform to the notion of SLOCC. They can therefore be represented in terms of their equivalence classes and can be visualized in three dimensions.

2.3 Lorentz Geometry of Two Qubits

To describe the SLOCC equivalence classes of qubits it is convenient to use their Lorentz description. Any single qubit observable Q can be written as

$$Q = q_\mu \sigma^\mu \tag{2.12}$$

The observable Q is then represented by the real 4-vector q.

Q is positive, and so is a state, if its trace and determinant are positive. Since $TrQ = 2q_0 > 0$ and $\det Q = q_\mu q^\mu \geq 0$, states are described by 4-vectors q that lie in the forward light-cone. Consider

$$Q^M = MQM^\dagger = q_\mu\,(M\sigma^\mu M^\dagger), \quad M \in SL(2,\mathbb{C}) \tag{2.13}$$

Since $q_\mu q^\mu = \det Q = \det Q^M$, it follows that the action of $M \in SL(2,\mathbb{C})$ on the observable Q can be implemented by an (orthochronous) Lorentz transformation of the four vector q. Namely, [32],

$$Q^M = q_\mu\,(M\sigma^\mu M^\dagger) = (\Lambda_M q)_\mu \sigma^\mu, \quad \Lambda_M \in SO_+(1,3) \tag{2.14}$$

Similarly, any observable W in the world of 2 qubits can be represented by a 4×4 real matrix ω as in Eq. (2.1). This representation allows a simple geometric characterization of potential entanglement witnesses in terms of matrices ω that map the forward light-cone into itself. This follows from the fact that W is an entanglement witness iff for any product state, represented by time-like vectors $\rho_a,\ \rho_b$:

$$Tr(W\rho_a \otimes \rho_b) = 4\omega_{\mu\nu}\rho_a^\mu \rho_b^\nu = 4\rho_a^\mu(\omega\rho_b)_\mu \geq 0 \tag{2.15}$$

This characterization of potential witnesses will play a role in the following.

To describe the SLOCC equivalence classes we shall consider invariants under the action (2.2). The pair $A, B \in SL(2,\mathbb{C})$ associated with $M = A \otimes B$ gives rise to a pair of Lorentz transformations Λ_A and Λ_B such that [20]:

$$\omega^M = \Lambda_A \omega \Lambda_B^T \tag{2.16}$$

Since $\det \Lambda_A = \det \Lambda_B = 1$, $\det \omega$ is an invariant.

A more interesting and powerful invariant is constructed as follows: The Minkowski adjoint of ω is defined as:

$$\omega^\star = \eta \omega^T \eta \tag{2.17}$$

where η is the Minkowski metric tensor. $\omega^\star$ transforms contragradiently to ω under M. This follows easily from the defining relations of the Lorentz transformation $\Lambda\eta\Lambda^T = \eta$:

$$\begin{aligned}(\omega^M)^\star &= \eta(\omega^M)^T\eta \\ &= \eta(\Lambda_A\omega\Lambda_B^T)^T\eta \\ &= (\eta\Lambda_B\eta)(\eta\omega^T\eta)(\eta\Lambda_A^T\eta) \\ &= (\Lambda_B^T)^{-1}\omega^\star(\Lambda_A)^{-1}\end{aligned} \tag{2.18}$$

It follows that $\omega^\star\omega$ undergoes a similarity transformation under the action of M, so its spectrum is a SLOCC invariant.

For a general observable, $\omega^\star\omega$ is not guaranteed to be a hermitian matrix, and its spectrum therefore may not be real. However, if W is a potential entanglement witness, a simplification occurs. In particular, the eigenvalues of $\omega^\star\omega$ are guaranteed to be positive [20, 19]. This can be seen from the following argument: Suppose W is a *strict* witness of entanglement, so that Eq. (2.15) holds with strict inequality. $\omega^\star\omega$ then maps the forward light-cone into its interior, since for any causal vector ρ

$$0 < (\omega\rho)_\mu(\omega\rho)^\mu = \rho_\mu(\omega^\star\omega\rho)^\mu \tag{2.19}$$

This implies, by a fixed point argument, that the largest eigenvalue of $\omega^\star\omega$ is positive and has a time-like eigenvector. The Lorentz orthogonal subspace to this eigenvector is a space-like invariant subspace. Restricted to this subspace, the Minkowsky adjoint coincides with the ordinary adjoint. This makes the remaining eigenvalues positive as well[4].

Up to sign the *Lorentz singular values* [20] are defined as the roots of the eigenvalues of $\omega^\star\omega$. We denote them by ω_α. They are the Lorentz analog of the singular values of a matrix[5]. As the above argument shows, the largest singular value which will be denoted ω_0 corresponds generically to a timelike eigenvector (and in degenerate cases to a null one) while $\omega_1, \omega_2, \omega_3$ generically correspond to a spacelike eigenvector (or possibly a null one in degenerate cases).

Defining ω_α as the square roots of the (necessarily positive) eigenvalues of $\omega^\star\omega$ still leaves a sign ambiguity. A unique determination of ω_α is achieved by letting ω_3 take the sign of $\det\omega$ and choosing all others non-negative. Furthermore, one orders them according to

$$\omega_0 \geq \omega_1 \geq \omega_2 \geq |\omega_3|, \quad sign(\omega_3) = sign(\det\omega) \tag{2.20}$$

Unless ω_0 happens to vanish the SLOCC equivalence class may be characterized, up to scaling, by the three vector

$$\vec{\omega} = \frac{1}{\omega_0}\big(\omega_1, \omega_2, \omega_3\big) \tag{2.21}$$

The SLOCC equivalence classes of potential entanglement witnesses would then be represented by the pyramid

$$\{(x, y, \pm z) \mid x \geq y \geq z \geq 0\} \tag{2.22}$$

Remarks:

- If W is a strict potential witness (implying $\omega_0 > |\omega_i|$) then it turns out [33] that in analogy to the usual singular value decomposition one can find a pair of Lorentz transformations that bring ω to its canonical form

  $$\sum \omega_\alpha \sigma^\alpha \otimes \sigma^\alpha \tag{2.23}$$

  This in turn implies that the singular values ω_α completely determine W's SLOCC equivalence class.

[4] If one replaces $<$ by $\leq$ above then it might happen that the largest eigenvalue has an eigenvector which is light-like. This case is much more complicated, but for our aims here can be handled by a limiting argument.

[5] ω_α are not the covariant components of a Lorenzian 4-vector.

- However, if $\omega_0 = max(|\omega_i|)$ (corresponding to a non-strict potential witness) then there is no a-priori guarantee that such a pair of Lorentz transformations exists. Witnesses W associated with this boundary case split into nonequivalent classes: those having the canonical form (2.23) and others having more complicated canonical forms [20]. Thus in the boundary case ω_α do not completely determine the SLOCC equivalence class.

Note that the condition $\omega_0 \geq |\omega_1|, |\omega_2|, |\omega_3|$ is enough to guarantee that $\omega = diag(\omega_0, \omega_1, \omega_2, \omega_3)$ takes the forward light-cone to itself and hence to guarantee that a potential entanglement witness $W = \sum \omega_\alpha \sigma^\alpha \otimes \sigma^\alpha$ having ω_α as singular values exists.

Operators $W = \sum \omega_\alpha \sigma^\alpha \otimes \sigma^\alpha$ which differ by permutation of $\omega_1, \omega_2, \omega_3$ or by flipping a sign of a pair of ω_i's are SLOCC equivalent. There are 24 such operations, corresponding to the tetrahedral group. Strictly, therefore, the SLOCC equivalence classes of W are represented by the pyramid of (2.20). However for the purpose of drawing pictures it is more aesthetic to symmetrize and give up (2.20). Now each (generic) equivalence class is represented by 24 points in the ω_i's space (2.21). In particular, the potential entanglement witnesses are then represented by the unit cube.

2.3.1 SLOCC and duality

The following fact [33] allows one to translate the duality relation between potential witnesses and separable states from 16 dimensions to 3:

Theorem 2.1. *Let W and W' be two potential entanglement witnesses. Then:*

$$\inf_{M,N} Tr(W^N W'^M) = 4\left(\omega_0\omega'_0 - \omega_1\omega'_1 - \omega_2\omega'_2 + \omega_3\omega'_3\right) \tag{2.24}$$

where ω_α and ω'_α are the Lorentz singular values of W and W' respectively, ordered according to Eq. (2.20).

From a geometric point of view it may be more aesthetic to use an equivalent formulation of the theorem which allows using any of the 24 possible representatives ω_α (not necessarily satisfying (2.20)). This is easily achieved by replacing the r.h.s. of Eq. (2.24) by

$$4 \min\left\{\omega_0\omega'_0 + \omega_1\omega'_1 + \omega_2\omega'_2 + \omega_3\omega'_3\right\}$$

where the minimum is taken over the 24 possible representatives ω'_α.

In particular, given a potential witness W and a separable state ρ_s, we have for any representative as in Eq. (2.21), $\vec{\omega}$ and $\vec{\rho}$, the inequality

$$0 \leq 4(1 + \vec{\omega} \cdot \vec{\rho}) \tag{2.25}$$

Fig. 10 demonstrates this inequality for a particular choice of W.

Since the positivity of the right hand side is the standard duality relation between convex sets in 3 dimensions [21], we see that the theorem translates the duality, Eq. (2.4), between the 16 dimensional cones, to the duality between convex sets in 3 dimensions [21].

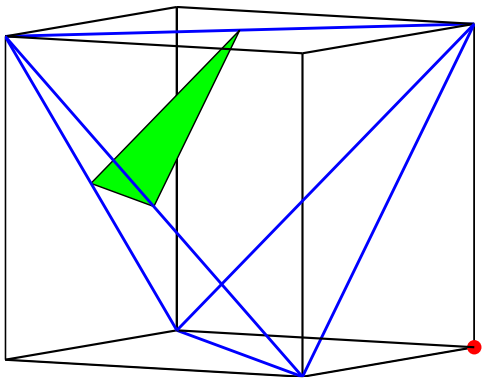

Figure 10: The red dot in the lower right corner is an entanglement witness associated with $\vec{\omega}$. The green triangle lies on the plane $\vec{\rho} \cdot \vec{\omega} = -1$. One may think of points near the corner of the tetrahedron that lie beyond the green triangle as representing the states that are incriminated as entangled by $\vec{\omega}$. The chosen witness is optimal in the sense that no other entanglement witness detects a larger set of entangled states.

Letting the tetrahedral group act on the pyramid of Eq. (2.22) gives the unit cube. Since the cube is the dual (also known as Polar [21]) of the octahedron, one learns from Eq. (2.25) that the SLOCC equivalence classes of the separable states are represented by the octahedron (up to the tetrahedral symmetries).

The 16 dimensional set of states is self-dual. By Eq. (2.25) the corresponding SLOCC equivalence classes must be represented by a self-dual convex set in three dimensions, which turns out to be the tetrahedron. To see this, note that an operator ρ in the canonical form, Eq. (2.23), is a sum of mutually commuting operators with one relation, $(\prod \sigma^\mu \otimes \sigma^\mu = -1)$. It follows that its eigenvalues are

$$\{\rho_0 + \epsilon_1\rho_1 + \epsilon_2\rho_2 - \epsilon_1\epsilon_2\rho_3\} \tag{2.26}$$

where $\epsilon_1, \epsilon_2 \in \{+1, -1\}$. Requiring ρ to be positive restricts it to the intersection of four half-spaces, which evidently yield the tetrahedron. This completes the derivation of Fig. 9.

One nice consequence of the geometric construction is a "proof by inspection" that for 2 qubits the Peres separability test is iff [19]. It is easy to see [6] that if ρ is a separable state, then its partial transpose is positive. The converse is not true in general, but is true for 2 qubits. However the proof [7] rests on non-elementary facts from operator algebras[6].

The proof by inspection goes as follows [19]: Denote by ρ^{pt} the partial transposition of ρ. Since σ_2 is antisymmetric, while the remaining σ_μ are symmetric, one has

$$(\rho^{pt})_{\mu\nu} = \begin{cases} -\rho_{\mu 2}, \text{ for } \nu = 2 \\ \rho_{\mu\nu}, \text{ otherwise} \end{cases} \tag{2.27}$$

On the SLOCC equivalence classes of states $\rho = \varrho_\alpha \sigma^\alpha \otimes \sigma^\alpha$, the partial transposition then acts as a reflection in the 2 axis: Replacing ϱ_2 with $-\varrho_2$, Since the octahedron of separable states is the intersection of the tetrahedron with its reflection through the $\varrho_2 = 0$ plane the result follows.

2.4 Visualizing the CHSH inequalities

The CHSH witnesses and inequalities were described in section 2.2.3. For the sake of simplicity in notation we shall now stick with the plus sign in the witness of Eq. (2.8)[7].

If a state violates a CHSH inequality then it is necessarily entangled, but the opposite claim is false; There are entangled states that do not violate any CHSH inequality. Our aim is to visualize these.

The CHSH witnesses have the property that $(\omega_B)_{0j} = (\omega_B)_{j0} = 0$. This family is invariant under the action of LOCC. The associated equivalence classes then live in three dimensions and are in 1-1 correspondence with the 3 singular values of the 3×3 matrix $\tilde{\omega}_B$

$$(\tilde{\omega}_B)_{ij} = (\omega_B)_{ij} \tag{2.28}$$

The singular values are the square roots of the three eigenvalues of $\tilde{\omega}_B^\dagger \tilde{\omega}_B$.

To find the explicit dependence of the singular values on the LOCC invariants $\cos\alpha = \hat{a} \cdot \hat{a}'$ and $\cos\beta = \hat{b} \cdot \hat{b}'$—the angles between the two directions Alice and Bob choose—we

[6] See [29] for the history of this problem.

[7] The minus sign corresponds to flipping $\hat{b}, \hat{b}'$.

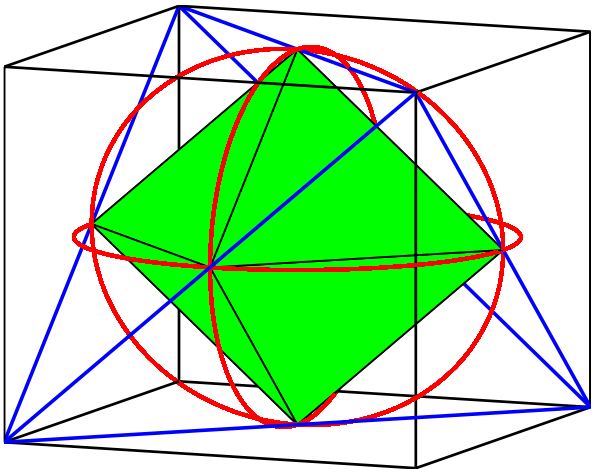

Figure 11: The circles represent the CHSH Witnesses

introduce the pair of 3×2 matrices:

$$A = \left(\hat{a}, \hat{a}'\right) \qquad B = \left(\hat{b}, \hat{b}'\right) \tag{2.29}$$

One checks that

$$2\tilde{\omega}_B = a \otimes (b + b')^T + a' \otimes (b - b')^T = A \begin{pmatrix} 1 & 1 \\ 1 & -1 \end{pmatrix} B^T \tag{2.30}$$

Since $\tilde{\omega}_B^\dagger \tilde{\omega}_B$ is manifestly a 3×3 matrix with rank 2, one of its eigenvalues is zero. Its remaining nonzero eigenvalues equal to those of the 2×2 matrix

$$\tfrac{1}{4}(B^T B) \begin{pmatrix} 1 & 1 \\ 1 & -1 \end{pmatrix} (A^T A) \begin{pmatrix} 1 & 1 \\ 1 & -1 \end{pmatrix} \tag{2.31}$$

Evidently

$$A^T A = \begin{pmatrix} 1 & \cos\alpha \\ \cos\alpha & 1 \end{pmatrix}, \quad B^T B = \begin{pmatrix} 1 & \cos\beta \\ \cos\beta & 1 \end{pmatrix} \tag{2.32}$$

The matrix in Eq. (2.31) now takes the form

$$\begin{pmatrix} \cos^2(\frac{\alpha}{2}) & \cos\beta \sin^2(\frac{\alpha}{2}) \\ \cos\beta \cos^2(\frac{\alpha}{2}) & \sin^2(\frac{\alpha}{2}) \end{pmatrix} \tag{2.33}$$

It has a unit trace, so the singular values of $\tilde{\omega}_B$ lie on the unit circle $\omega_1^2 + \omega_2^2 = 1,\ \omega_3 = 0$. Solving for the eigenvalues we find:

$$2\omega_{1,2}^2 = 1 \pm \sqrt{1 - \sin^2\alpha \sin^2\beta},\ \omega_3 = 0$$

As α and β vary from 0 to 2π this gives one eighth of the unit circle where $1 \geq \omega_1 \geq \omega_2 \geq 0$. If we adjoin to it the twenty four representatives of the same equivalence class, we get the three mutually intersecting unit circles, shown in Fig. 11, representing the LOCC equivalence classes of CHSH witnesses.

The dual set to the three unit circles (more precisely, to their convex hull) then represents the LOCC equivalence classes of the states that satisfy all the CHSH inequalities[8]. To describe this geometrically, note that the dual set of the unit circle in the $x - y$ plane, for example, is the cylinder along the z axis, with a unit radius. The LOCC equivalence classes of states that satisfy all the CHSH inequalities is the intersection of three cylinders along the x, y and z axes, with a unit radius. This set (see Figure 12) is bigger than the set of separable states represented by the octahedron.

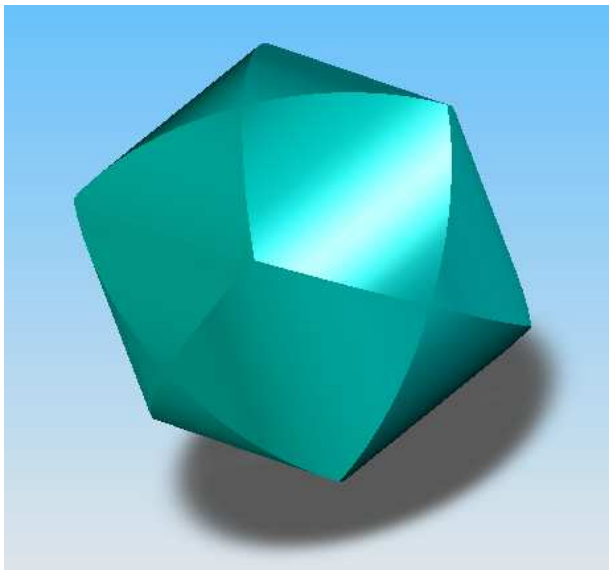

Figure 12: The set of states that satisfy all CHSH inequalities in the SLOCC sense is the intersection of three cylinders.

[8]A-priori, only states with completely mixed subsystems are accommodated in a 3-D LOCC diagram. However, it is easy to see that ρ_{0j} and ρ_{j0} do not affect $Tr(\rho W_B)$.

2.4.1 Optimizing the CHSH Inequality

In [34] R. Horodecki, P. Horodecki and M. Horodecki solved the problem of finding the optimal CHSH witness[9] for a given (normalized) state ρ. They show that

$$\tfrac{1}{4}Tr(\rho W_B) \geq 1 - \sqrt{\rho_1^2 + \rho_2^2} \tag{2.34}$$

and the inequality is saturated for an appropriate choice of angles α, β. Here $\rho_{1,2}$ are the two largest singular values of the 3×3 matrix $\tilde{\rho}$ constructed from the spatial components of the matrix elements $\rho_{\mu\nu}$ as in Eq. (2.28). In particular, the state ρ violates a CHSH inequality if and only if $\rho_1^2 + \rho_2^2 > 1$.

This result can be derived, essentially by inspection, from the geometric description of the previous section. Recall (see footnote 8) that the state ρ may be assumed, without loss of generality, to be one where the subsystems are completely mixed. The LOCC equivalence class of ρ is represented by the three singular values of $\tilde{\rho}$, which we denote by $\vec{\rho}$. A Bell witness is represented by the three singular values of $\tilde{\omega}_B$, which we denote by $\vec{\omega}_B$. The vector $\vec{\omega}_B$ takes values on the three circles in the figure. For a normalized state ρ

$$\tfrac{1}{4}Tr(\rho W_B) = 1 + \vec{\rho} \cdot \vec{\omega}_B \tag{2.35}$$

It is clear that the optimal choice of a witness (a minimizer) is to choose the witness $\tilde{\omega}_B$ so that the vector $\vec{\omega}_B$ is as anti-parallel to $\vec{\rho}$ as possible. (Recall that $\vec{\omega}_B$ is constrained to lie in one of the principal planes.) The minimizer is then the smallest entry among

$$\{1 - |\vec{\rho} \times \hat{x}|\,, 1 - |\vec{\rho} \times \hat{y}|\,, 1 - |\vec{\rho} \times \hat{z}|\} \tag{2.36}$$

This reproduces the result of Horodecki et al.

2.4.2 SLOCC interpretation

Fig. 12 also admits the following SLOCC interpretation: The states represented by points lying in the intersection of the three cylinders have the property that they, and all that can be filtered from them, satisfy all the CHSH inequalities. This is an immediate consequence of theorem 2.1 which guarantees that $Tr(\rho^{A\otimes B} W_B)$ attains its minimum value when ρ takes its canonical form.

The SLOCC equivalence classes of states that lie outside the intersection of the cylinders have the property that they can always be filtered to yield states that violate some CHSH inequality.

[9] See also [35].

2.5 More can be less

The CHSH inequality constrains Alice and Bob to two dichotomic tests each. A general theory of Bell inequalities allows Alice and Bob n_A and n_B tests, having m_A and m_B possible results. (A geometric framework for deriving such generalized Bell inequalities is described in [11].) Let $I(n_A n_B m_A m_B)$ denote a corresponding Bell inequality. The CHSH inequality is then $I(2222)$. Von Neumann tests on qubits restrict the outcomes of each test to two, $m_A = m_B = 2$; however, the number of tests, n_A, n_B can be arbitrary.

One naively expects that by increasing the number of tests one might be able to incriminate some of the entangled states that pass the CHSH test. Indeed, D. Collins and N. Gisin [17] present an example of a state ρ that violates an $I(3322)$ inequality but does not violate any CHSH inequality.

Here we shall present numerical evidence which shows that when Bell inequalities are interpreted in the SLOCC sense, then $I(3322)$ (with three dichotomic tests) is strictly weaker than $I(2222)$. It follows that the state found by Collins and Gisin can be filtered to a state that violates CHSH.

The $I(3322)$ inequality derived by D. Collins and N. Gisin [17] takes the form

$$\begin{aligned} &-2P(B_1) - P(B_2) - P(A_1) + P(A_1B_1) + P(A_1B_2) + P(A_1B_3) + \\ &P(A_2B_1) + P(A_2B_2) - P(A_2B_3) + P(A_3B_1) - P(A_3B_2) \leq 0 \end{aligned} \tag{2.37}$$

where $P(A_iB_j)$ is the probability that when Alice chooses the ith measurement and Bob chooses the jth measurement, they both get the outcome 0.

Allowing Alice and Bob three experiments to choose from gives them more freedom. In particular, they are always free to disconnect the third experiment. This means that the CHSH, or $I(2222)$, must be a special case of $I(3322)$. Indeed, the CHSH $I(2222)$ inequality,

$$P(A_1B_1) + P(A_1B_2) + P(A_2B_1) - P(A_2B_2) - P(B_1) - P(A_1) \leq 0 \tag{2.38}$$

is obtained from $I(3322)$ by Alice disconnecting her third experiment, $P(A_3) = 0$, and Bob disconnecting his first experiment, $P(B_1) = 0$. Renaming B_2 and B_3 as B_1 and B_2 respectively gives CHSH.

Dichotomic, von Neumann, tests of Alice and Bob are described by projection operators, namely setting in the above

$$P(A_iB_j) \to \frac{1 + a_i \cdot \sigma}{2} \otimes \frac{1 + b_j \cdot \sigma}{2} \tag{2.39}$$

where a_i and b_j are interpreted as directions in a measurement of the spin projection. Note that the case of a disconnected experiment *is not* of this form: It is not a dichotomic von Neumann measurement.

The witness corresponding to $I(3322)$ with three dichotomic von Neumann measurements for both Alice and Bob is then

$$\begin{aligned} W_{3322} = & 4I \otimes I + I \otimes (b_1 + b_2) \cdot \sigma - (a_1 + a_2) \cdot \sigma \otimes I \\ & - (a_1 + a_2) \cdot \sigma \otimes (b_1 + b_2) \cdot \sigma \ - (a_1 - a_2) \cdot \sigma \otimes b_3 \cdot \sigma \\ & - a_3 \cdot \sigma \otimes (b_1 - b_2) \cdot \sigma \end{aligned} \tag{2.40}$$

$Tr\,(\rho W_{3322}) < 0$ implies that the state ρ violates a Bell inequality.

W_{3322} represents an (a-priori) 12 dimensional family of witnesses. It has six LOCC invariant parameters, the angles $\cos(\alpha_{ij}) = a_i \cdot a_j$ and $\cos(\beta_{ij}) = b_i \cdot b_j$, $i \neq j \in \{1, 2, 3\}$. We can visualize this family in 3 dimensions by representing $W_{3322} = (\omega_{3322})_{\mu\nu}\sigma^\mu \otimes \sigma^\nu$ by its canonical form under $SL(2, \mathbb{C})$.

Let us introduce the following direction matrices

$$A = \begin{pmatrix} 1 & 0 & 0 & 0 \\ 0 & a_{1x} & a_{2x} & a_{3x} \\ 0 & a_{1y} & a_{2y} & a_{3y} \\ 0 & a_{1z} & a_{2z} & a_{3z} \end{pmatrix} \quad B = \begin{pmatrix} 1 & 0 & 0 & 0 \\ 0 & b_{1x} & b_{2x} & b_{3x} \\ 0 & b_{1y} & b_{2y} & b_{3y} \\ 0 & b_{1z} & b_{2z} & b_{3z} \end{pmatrix} \tag{2.41}$$

and

$$W_0 = \begin{pmatrix} 4 & -1 & -1 & 0 \\ 1 & -1 & -1 & -1 \\ 1 & -1 & -1 & 1 \\ 0 & -1 & 1 & 0 \end{pmatrix} \tag{2.42}$$

so $\omega_{3322} = AW_0B^T$. The Lorentz singular values are the roots of the eigenvalues of $(B^T\eta B)W_0^T(A^T\eta A)W_0$. One finds

$$A^T\eta A = \begin{pmatrix} 1 & 0 & 0 & 0 \\ 0 & -1 & -\cos(\alpha_{12}) & -\cos(\alpha_{13}) \\ 0 & -\cos(\alpha_{12}) & -1 & -\cos(\alpha_{23}) \\ 0 & -\cos(\alpha_{13}) & -\cos(\alpha_{23}) & -1 \end{pmatrix} \tag{2.43}$$

$$B^T \eta B = \begin{pmatrix} 1 & 0 & 0 & 0 \\ 0 & -1 & -\cos(\beta_{12}) & -\cos(\beta_{13}) \\ 0 & -\cos(\beta_{12}) & -1 & -\cos(\beta_{23}) \\ 0 & -\cos(\beta_{13}) & -\cos(\beta_{23}) & -1 \end{pmatrix} \tag{2.44}$$

The Lorentz singular values were calculated numerically. The intersection of the resulting set with the $X-Y$ plane, shown in Fig. 13, is clearly contained in the CHSH unit circle. Similarly all points outside this plane were found to lie inside the convex hull of the three CHSH circles, implying that they represent weaker witnesses. This means that under SLOCC the CHSH inequality is stronger than I_{3322} (when Alice and Bob are constrained to measure three spin directions).

Thus, if the two parties are allowed to filter, then by letting them choose from 3 possible experiments, we gain less information than by restricting them to choose from 2 possible experiments.

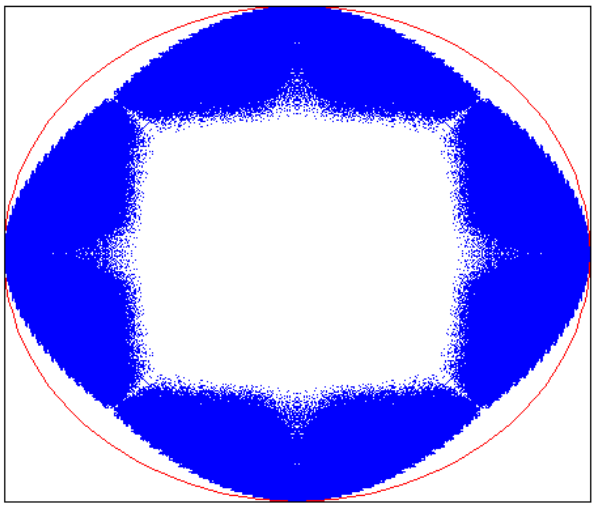

Figure 13: CHSH and I_{3322} Witnesses in the $X-Y$ plane: the circle represents CHSH witnesses while all the dots inside represent I_{3322} witnesses in this plane. Since the dots lie inside the circle they represent weaker witnesses.

3 Measuring Entanglement Witness

3.1 Introduction

Manufacturing entangled states in the lab is highly important for quantum information [1]. In order to prove the existence of entanglement, one can measure the entire quantum state using tomography techniques. In the case of two qubits, the 4×4 density matrix is positive semi-definite, Hermitian, and with unit trace. Thus, finding the state requires 16 linearly independent measurements, where one is for normalization. The measurements we use consist of products of two local projective measurements. After reconstructing the density matrix, the Peres test [6, 7] can be used to check whether the state is entangled or not.

We want to develop tools that can effectively tell, using as few measurements as possible, if a quantum state is entangled or not, without having to reconstruct the entire density matrix. In light of theorem 1.1, one can measure an entanglement witness instead of finding the state, and reduce the number of measurements needed. Every entangled state has a corresponding witness which detects it, and states in its neighborhood, as entangled, but there is no universal witness. In order to prove entanglement we need to choose a suitable witness to measure.

In this work, we introduce an entangled mixed state, motivated by [36], and its corresponding witness. This state is a result of a cascade of a four level quantum system with two intermediate levels. The two different decay channels produce $|H\rangle$ and $|V\rangle$ polarized photons, respectively (see Fig. 14).

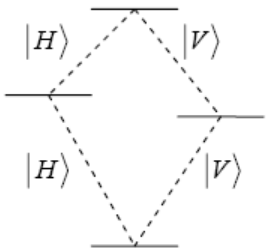

Figure 14: Four level quantum system with two intermediate levels. There are two possible decay channels. One channel produces $|H\rangle$ polarized photons, while the other channel produces $|V\rangle$ polarized photons

The wave function of the photon pair, assuming that the final state of the system is

the same for both of the decay channels, is:

$$|\psi\rangle = \alpha|HH\rangle|P_H\rangle + \beta|VV\rangle|P_V\rangle \tag{3.1}$$

Where $|\alpha|^2 + |\beta|^2 = 1$ and $|P_H\rangle$, $|P_V\rangle$ are the wave packets of the photons.
The polarization density matrix after tracing out the wave packets is:

$$\rho = \begin{pmatrix} |\alpha|^2 & 0\ 0 & re^{i\phi} \\ 0 & 0\ 0 & 0 \\ 0 & 0\ 0 & 0 \\ re^{-i\phi} & 0\ 0 & |\beta|^2 \end{pmatrix}; \qquad r > 0, \tag{3.2}$$

where $re^{i\phi} = \alpha\beta^*\langle P_V|P_H\rangle$.

The measurements needed for the entanglement witness are given for couple of cases. In section 3.4.1, we restrict the allowed measurements to the standard set of:

$$\begin{aligned} |H\rangle &= |0\rangle \\ |V\rangle &= |1\rangle \\ |D\rangle &= \tfrac{1}{\sqrt{2}}(|H\rangle + |V\rangle) \\ |\bar{D}\rangle &= \tfrac{1}{\sqrt{2}}(|H\rangle - |V\rangle) \\ |L\rangle &= \tfrac{1}{\sqrt{2}}(|H\rangle + i|V\rangle) \\ |R\rangle &= \tfrac{1}{\sqrt{2}}(|H\rangle - i|V\rangle) \end{aligned} \tag{3.3}$$

In section 3.4.2, we assume that all measurements are allowed in the lab, meaning that any polarization can be measured. Our goal is to find the minimal number of local projective measurements required for measuring the expectation value of the witness.

3.2 Review of Two Qubits Tomography

In order to measure a density matrix, 16 independent measurements are needed. We use projective measurements $\{P_\mu\}_{\mu=1}^{16}$, where each of the measurements is a product of two local projective measurements:

$$P_\mu = |p_\mu^{(1)}\rangle\langle p_\mu^{(1)}| \otimes |p_\mu^{(2)}\rangle\langle p_\mu^{(2)}| \tag{3.4}$$

Following the notation of James et al. [37], we introduce a set of 16 linearly independent 4×4 matrices Γ_μ, that are orthonormal with respect to the trace inner product

$\langle A, B\rangle = Tr(A^\dagger B)$ (see appendix A). By definition, for every 4×4 matrix ρ, we have:

$$\rho = \sum_{\mu=1}^{16} \langle \Gamma_\mu, \rho \rangle \Gamma_\mu \tag{3.5}$$

For a complete set of 16 projective measurements $\{P_\mu\}$, we define a 16×16 matrix B, such that

$$B_{\mu\nu} = Tr(P_\mu \Gamma_\nu) \tag{3.6}$$

The outcomes of the measurements of a density matrix ρ are:

$$n_\mu = N\, Tr(P_\mu \rho) = N \sum_{\nu=1}^{16} Tr(P_\mu \Gamma_\nu) Tr(\Gamma_\nu \rho) = N \sum_{\nu=1}^{16} B_{\mu\nu} Tr(\Gamma_\nu \rho) \tag{3.7}$$

where N is a positive constant depending on the flux of photons and is used for normalization of the density matrix [37].

By inverting Eq. (3.7):

$$Tr(\Gamma_\mu \rho) = \frac{1}{N} \sum_{\nu=1}^{16} (B^{-1})_{\mu\nu} n_\nu \tag{3.8}$$

Substituting this into (3.5) and defining the 4×4 matrices $M_\nu = \sum_{\mu=1}^{16} \Gamma_\mu (B^{-1})_{\mu\nu}$, we have:

$$\rho = \frac{1}{N} \sum_{\mu,\nu=1}^{16} \Gamma_\mu (B^{-1})_{\mu\nu} n_\nu = \frac{1}{N} \sum_{\nu=1}^{16} M_\nu n_\nu \tag{3.9}$$

In order to measure an entanglement witness $\langle W \rangle$:

$$Tr(W\rho) = \frac{1}{N} \sum_{\nu=1}^{16} Tr(W M_\nu) n_\nu \tag{3.10}$$

From Eq. (3.10) we see that not all 16 measurements are necessarily needed. The measurement P_ν is needed only if $Tr(W M_\nu) \neq 0$. Since we are interested only in the sign of $Tr(W\rho)$, we do not need to find[10] the constant N.

3.3 Mutually Unbiased Bases

A density matrix of a quantum state in a Hilbert of d dimensions has $d^2 - 1$ parameters. Let $M = \sum_m m P_m$ be a projective measurement, such that $\sum_m P_m = I$ and

[10]The constant N is important if one wants to know not only whether the state is entangled or not, but also how much entanglement there is.

$P_m P_{m'} = \delta_{mm'} P_m$. There are at most d eigenspaces of M, providing $d-1$ independent probabilities. Thus, in order to determine the complete density matrix, one needs $d+1$ projective measurements. An optimal choice of the measurements would be a set of mutually unbiased bases (MUB) [38].

Definition 3.1. *Let $\{\mathcal{B}_k\}_{k=1}^m$ be a set of orthonormal bases $\mathcal{B}_k = \{|\psi_1^k\rangle, .., |\psi_d^k\rangle\}$, such that*

$$|\langle\psi_i^l|\psi_j^k\rangle| = \frac{1}{\sqrt{d}}$$

for every $i, j = 1, .., d$ and $l, k = 1, .., m$ where $l \neq k$. $\{\mathcal{B}_k\}_{k=1}^m$ is a set of mutually unbiased bases.

MUB are optimal in the sense that the different measurements have minimal overlap between them, so every measurement adds the maximum of new information possible. In the case $d = 4$, one can find 5 mutually unbiased bases, but only 3 mutually unbiased bases of separable states. The remaining 2 are entangled states.

Here are two examples of 3 mutually unbiased bases of separable states for the case $d = 4$:

$$\begin{aligned}
\mathcal{B}_1 &= \{|HH\rangle, |HV\rangle, |VH\rangle, |VV\rangle\} \\
\mathcal{B}_2 &= \{|DD\rangle, |D\bar{D}\rangle, |\bar{D}D\rangle, |\bar{D}\bar{D}\rangle\} \\
\mathcal{B}_3 &= \{|LL\rangle, |LR\rangle, |RL\rangle, |RR\rangle\}
\end{aligned} \tag{3.11}$$

and:

$$\begin{aligned}
\mathcal{B}_1 &= \{|HH\rangle, |HV\rangle, |VH\rangle, |VV\rangle\} \\
\mathcal{B}_2 &= \{|LD\rangle, |L\bar{D}\rangle, |RD\rangle, |R\bar{D}\rangle\} \\
\mathcal{B}_3 &= \{|DL\rangle, |DR\rangle, |\bar{D}L\rangle, |\bar{D}R\rangle\}
\end{aligned} \tag{3.12}$$

In this work, we are interested in *product* projective measurement, so we cannot find mutually unbiased bases for a complete determination of the state.

3.4 Measurements of the Witness

Let us introduce a family of states:

$$|e(\theta)\rangle = \frac{1}{\sqrt{2}}\big(e^{i\theta}|01\rangle - |10\rangle\big) \tag{3.13}$$

And a corresponding family of operators:

$$W(\theta) = \big(|e(\theta)\rangle\langle e(\theta)|\big)^{pt} = \frac{1}{2}\begin{pmatrix} 0 & 0\,0 & -e^{i\theta} \\ 0 & 1\,0 & 0 \\ 0 & 0\,1 & 0 \\ -e^{-i\theta} & 0\,0 & 0 \end{pmatrix} \tag{3.14}$$

where A^{pt} denotes the partial transposition of the matrix A of the second subsystem. For a legitimate one qubit state ρ_B, its transposition ρ_B^T is also a state. For a product state $\rho = \rho_A \otimes \rho_B$, its partial transposition $\rho^{pt} = \rho_A \otimes \rho_B^T$ is also a state. Thus, the following holds for all product states:

$$Tr\{W(\theta)\rho_A \otimes \rho_B\} = \langle e(\theta)|\rho_A \otimes \rho_B^T|e(\theta)\rangle \geq 0 \tag{3.15}$$

since the matrix $\rho_A \otimes \rho_B^T$ is positive semi definite. The expectation value of $W(\theta)$ for the state (3.2) is

$$Tr\{\rho W(\theta)\} = -r\cos(\phi - \theta) \tag{3.16}$$

Thus, the operators (3.14) are entanglement witnesses.

The partial transposition of the state (3.2), which is denoted as ρ^{pt}, has a negative eigenvalue, $-r$, with a corresponding eigenvector $|e(\phi)\rangle$. Thus, the state (3.2) is entangled following the Peres criterion [6, 7]. We see that $W(\phi)$ is the preferred entanglement witness for the state (3.2), since $Tr(\rho W(\phi)) = -r$.

The entanglement witness (3.14) can also detect states in the neighborhood of (3.2). If we add some random noise $\rho' = (1-\epsilon)\rho + \frac{1}{4}\epsilon I$ then:

$$Tr\{\rho' W(\theta)\} = -(1-\epsilon)r\cos(\phi - \theta) + \frac{1}{4}\epsilon \tag{3.17}$$

So the better we tune the phase θ of the witness closer to the phase ϕ of the state, the better can we detect noisy states as entangled.

3.4.1 Measuring only with the Standard Set

Suppose that only the measurement H, V, D, $\bar{D}$, L and R can be used. These measurements are somewhat more common and standard. With the 16 measurements in table 1,

μ	$\lvert p_\mu^{(1)}\rangle$	$\lvert p_\mu^{(2)}\rangle$
1	$\lvert H\rangle$	$\lvert H\rangle$
2	$\lvert H\rangle$	$\lvert V\rangle$
3	$\lvert V\rangle$	$\lvert H\rangle$
4	$\lvert V\rangle$	$\lvert V\rangle$
5	$\lvert L\rangle$	$\lvert \bar{D}\rangle$
6	$\lvert R\rangle$	$\lvert D\rangle$
7	$\lvert D\rangle$	$\lvert L\rangle$
8	$\lvert \bar{D}\rangle$	$\lvert R\rangle$
9	$\lvert D\rangle$	$\lvert D\rangle$
10	$\lvert \bar{D}\rangle$	$\lvert \bar{D}\rangle$
11	$\lvert L\rangle$	$\lvert L\rangle$
12	$\lvert R\rangle$	$\lvert R\rangle$
13	$\lvert D\rangle$	$\lvert H\rangle$
14	$\lvert H\rangle$	$\lvert D\rangle$
15	$\lvert H\rangle$	$\lvert L\rangle$
16	$\lvert R\rangle$	$\lvert H\rangle$

Table 1: A complete set of 16 measurements $P_\mu = |p_\mu^{(1)} p_\mu^{(2)}\rangle\langle p_\mu^{(1)} p_\mu^{(2)}|$ using the standard polarization basis.

we can measure the expectation value of $W(\theta)$ for 4 different values of the phase θ:

$$\begin{aligned} W(0) &= \{P_2 + P_3 - (P_9 + P_{10} - P_{11} - P_{12})\} \\ W\left(\tfrac{\pi}{2}\right) &= \{P_2 + P_3 - (P_5 + P_6 - P_7 - P_8)\} \\ W(\pi) &= \{P_2 + P_3 + (P_9 + P_{10} - P_{11} - P_{12})\} \\ W\left(\tfrac{3\pi}{2}\right) &= \{P_2 + P_3 + (P_5 + P_6 - P_7 - P_8)\} \end{aligned} \tag{3.18}$$

Eq. (3.18) indicates that for the witness $W(0)$ for example, $Tr(WM_\nu) \neq 0$ for $\nu = 2, 3, 9, 10, 11, 12$. Thus, as was explained at the end of section 3.2, in order to find the sign of $Tr(\rho W(0))$ only 6 measurements are needed.

If the phase of the state ϕ is unknown, we need 10 measurements $\{P_2, P_3, P_5, .., P_{12}\}$ (see table 1) and by using Eq. (3.16) we can find the 4 expectation values:

$$\begin{aligned} Tr\left(\rho W\left(0\right)\right) &= -r\cos\left(\phi\right) \\ Tr\left(\rho W\left(\tfrac{\pi}{2}\right)\right) &= -r\cos\left(\phi - \tfrac{\pi}{2}\right) \\ Tr\left(\rho W\left(\pi\right)\right) &= -r\cos\left(\phi - \pi\right) \\ Tr\left(\rho W\left(\tfrac{3\pi}{2}\right)\right) &= -r\cos\left(\phi - \tfrac{3\pi}{2}\right) \end{aligned} \tag{3.19}$$

One of the above is negative, which proves that the state is entangled.

If the phase of the state ϕ is known, we can choose only 6 measurements. We need to measure the expectation value of $W(\theta)$ such that $|\theta - \phi|$ is minimal. After choosing the phase $\theta = 0$, $\frac{\pi}{2}$, π, or $\frac{3\pi}{2}$, we can find the 6 measurements needed according to Eq. (3.18).

One may note that the 6 measurements needed for each entanglement witness in Eq. (3.18) belong to three mutually unbiased bases. The measurements of $W(0)$ and $W(\pi)$ are taken from the bases listed in Eq. (3.11): $P_2, P_3 \in \mathcal{B}_1$, $P_9, P_{10} \in \mathcal{B}_2$ and $P_{11}, P_{12} \in \mathcal{B}_3$. Similarly, the measurements of $W(\frac{\pi}{2})$ and $W(\frac{3\pi}{2})$ are taken from the bases listed in Eq. (3.12).

3.4.2 All Measurements are Allowed

Following the work of A. Sanpera et al. [39], O. Gühne et al. [40] gave a minimal decomposition to sum of products of $(|\varphi\rangle\langle\varphi|)^{pt}$, where $|\varphi\rangle = \alpha|00\rangle + \beta|11\rangle$ with α, β real, such that $\alpha^2 + \beta^2 = 1$. The minimal decomposition consists of 5 terms of product projections. The situation is different here, since the coefficients of the entanglement witness (3.14) are not real.

Let us define the following:

$$\begin{aligned} |f_1\rangle &= \tfrac{1}{\sqrt{2}}\left(e^{-i\pi/3}|H\rangle + ie^{-i\theta/2}e^{i\pi/3}|V\rangle\right) \\ |f_2\rangle &= \tfrac{1}{\sqrt{2}}\left(e^{i\pi/3}|H\rangle + ie^{-i\theta/2}e^{-i\pi/3}|V\rangle\right) \\ |f_3\rangle &= |f_1\rangle + |f_2\rangle \end{aligned} \tag{3.20}$$

μ	$\lvert p_\mu^{(1)}\rangle$	$\lvert p_\mu^{(2)}\rangle$
1	$\lvert H\rangle$	$\lvert H\rangle$
2	$\lvert V\rangle$	$\lvert V\rangle$
3	$\lvert f_1\rangle$	$\lvert f_2\rangle$
4	$\lvert f_2\rangle$	$\lvert f_1\rangle$
5	$\lvert f_3\rangle$	$\lvert f_3\rangle$

Table 2: The 5 measurements needed for the decomposition of $W(\theta)$, $P_\mu = |p_\mu^{(1)}p_\mu^{(2)}\rangle\langle p_\mu^{(1)}p_\mu^{(2)}|$. $|f_j\rangle$ are defined in (3.20)

With these notations and those of table 2, we have:

$$W(\theta) = \left\{\tfrac{2}{3}\left(P_3 + P_4 + P_5\right) - \tfrac{1}{2}\left(P_1 + P_4\right)\right\} \tag{3.21}$$

We see immediately from Eq. (3.21) that if the phase ϕ of the state (3.2) is known, and we can use the measurements listed in table 2, we need a total of 5 measurements in order to find the sign of the expectation value of $W(\phi)$ and to prove entanglement.

4 Summary

Many of the important concepts in quantum information, such as entangled and separable states, entanglement witnesses, the CHSH Bell inequalities, etc., can be visualized in three dimensions by introducing an appropriate equivalence relation. The visualization allows us to give a "proof by inspection" of the non-elementary fact [7] that the Peres separability test for 2 qubits is iff. It also allows us to "solve by inspection" the problem of optimizing the CHSH Bell inequality, which was solved by analytical methods in [34].

We have introduced the notion of states that satisfy Bell inequalities in the SLOCC sense. We gave numerical evidence which showed that allowing Alice and Bob an additional *dichotomic von Neumann* test does not enable them to shrink the set shown in Fig. 12, obtained by filtering and CHSH. It is an interesting open question whether four or more dichotomic tests, or more general POVM tests, can further shrink the set shown in Fig. 12.

In this work, we have given a recipe for measuring entanglement witnesses, minimizing the number of measurements needed. The state was assumed to be a general state (3.2), not necessarily pure, with a phase, not necessarily known. In case we use only the standard measurements $\{H, V, D, \bar{D}, L, R\}$, we need 10 measurements if the phase of the state is unknown and 6 measurements if the phase of the state is known. If we know the phase and we allow all measurements, we can further improve the result and use only 5 measurements in order to prove the existence of entanglement.

A Gamma matrices

Here we give a set of 16 linearly independent 4×4 matrices Γ_μ, with the property:

$$Tr(\Gamma_\mu \Gamma_\nu) = \delta_{\mu\nu} \tag{A.1}$$

This set spans the space of 4×4 matrices.

$$\begin{array}{llll} \Gamma_1 = \frac{1}{2} I \otimes I & \Gamma_2 = \frac{1}{2} I \otimes \sigma_x & \Gamma_3 = \frac{1}{2} I \otimes \sigma_y & \Gamma_4 = \frac{1}{2} I \otimes \sigma_z \\ \Gamma_5 = \frac{1}{2} \sigma_x \otimes I & \Gamma_6 = \frac{1}{2} \sigma_x \otimes \sigma_x & \Gamma_7 = \frac{1}{2} \sigma_x \otimes \sigma_y & \Gamma_8 = \frac{1}{2} \sigma_x \otimes \sigma_z \\ \Gamma_9 = \frac{1}{2} \sigma_y \otimes I & \Gamma_{10} = \frac{1}{2} \sigma_y \otimes \sigma_x & \Gamma_{11} = \frac{1}{2} \sigma_y \otimes \sigma_y & \Gamma_{12} = \frac{1}{2} \sigma_y \otimes \sigma_z \\ \Gamma_{13} = \frac{1}{2} \sigma_z \otimes I & \Gamma_{14} = \frac{1}{2} \sigma_z \otimes \sigma_x & \Gamma_{15} = \frac{1}{2} \sigma_z \otimes \sigma_y & \Gamma_{16} = \frac{1}{2} \sigma_z \otimes \sigma_z \end{array} \tag{A.2}$$

B Matlab Program for calculating M matrices

Here is a Matlab code that calculates the M-matrices.

```
%%%%%%%%%%%%%%%%%%%%%%%%%%%%%%%%%%%%%%%%%%%%%%%%%%%%%%%%%%%%%%%%%%%%%%%%
%% Definition of |H>, |V>, |D>, |Dbar>, |L> and |R> %%
%% Notations: |H>=z_p   |V>=z_m    %%%%%%%%%%%%%%%%%%%
%%%%%%%%%%%% |D>=x_p   |Dbar>=x_m %%%%%%%%%%%%%%%%%%%
%%%%%%%%%%%% |L>=y_p   |R>=ym     %%%%%%%%%%%%%%%%%%%
%%%%%%%%%%%%%%%%%%%%%%%%%%%%%%%%%%%%%%%%%%%%%%%%%%%%%%%%%%%%%%%%%%%%%%%%

%% Choose alpha: %%
alpha=0* pi/180;

%% Choose phase: %%
alpha=0* pi/180;

z_p=[1;0]; z_m=[0;1];%
f1=1/sqrt(2)*(exp(-i*pi/3)*z_p+exp(-i*alpha/2)*exp(i*pi/3)*z_m);%
f2=1/sqrt(2)*(exp(i*pi/3)*z_p+exp(-i*alpha/2)*exp(-i*pi/3)*z_m);%
f3=f1+f2;%
f4=1/sqrt(2)*(exp(-i*pi/3)*z_p
    +exp(-i*pi/4)*exp(-i*alpha/2)*exp(i*pi/3)*z_m);%
```

```
f5=1/sqrt(2)*(exp(i*pi/3)*z_p
    +exp(-i*pi/4)*exp(-i*alpha/2)*exp(-i*pi/3)*z_m);%
f6=f4+f5;%
x_p=1/sqrt(2)*[1; 1]; x_m=1/sqrt(2)*[1; -1];%
y_p=1/sqrt(2)*[1;i]; y_m=1/sqrt(2)*[1; -i];%

%%%%%%%%%%%%%%%%%%%%%%%%%%%%%%%%%%%%%%%%%%%%%%%%%%%%%%
%% Definition of projections of one qubit %%%%%%%%%%%
%% |H><H|=zp, |V><V|=zm,      %%%%%%%%%%%%%%%%%%%%%%%%
%% |D><D|=xp, |Dbar><Dbar|=xm %%%%%%%%%%%%%%%%%%%%%%%%
%% |L><L|=yp and |R><R|=ym    %%%%%%%%%%%%%%%%%%%%%%%%
%%%%%%%%%%%%%%%%%%%%%%%%%%%%%%%%%%%%%%%%%%%%%%%%%%%%%%

xp=(x_p*x_p'); xm=(x_m*x_m'); yp=(y_p*y_p'); ym=(y_m*y_m');
zp=(z_p*z_p'); zm=(z_m*z_m'); F1=(f1*f1'); F2=(f2*f2'); F3=(f3*f3');
F4=(f4*f4'); F5=(f5*f5');F6=(f6*f6');

%%%%%%%%%%%%%%%%%%%%%%%%%%%%%%%%%%%%%%%%%%%%%%%%%%%%%%
%% Definition of projections of two qubits %%%%%%%%%%
%% HH HV VH VV      .....      %%%%%%%%%%%%%%%%%%%%%%%%
%% DD DDbar DbarD DbarDbar .....  %%%%%%%%%%%%%%%%%%%%
%% LL LR RL RR  .....          %%%%%%%%%%%%%%%%%%%%%%%%
%%%%%%%%%%%%%%%%%%%%%%%%%%%%%%%%%%%%%%%%%%%%%%%%%%%%%%

HH=kron(zp,zp); HV=kron(zp,zm); VH=kron(zm,zp); VV=kron(zm,zm);
HD=kron(zp,xp); HL=kron(zp,yp); HDbar=kron(zp,xm); HR=kron(zp,ym);
DH=kron(xp,zp); LH=kron(yp,zp); VDbar=kron(zm,xm); VR=kron(zm,ym);
VD=kron(zm,xp); VL=kron(zm,yp); DV=kron(xp,zm); LV=kron(yp,zm);
DbarH=kron(xm,zp); RH=kron(ym,zp); DbarV=kron(xm,zm);
RV=kron(ym,zm); DD=kron(xp,xp); DbarDbar=kron(xm,xm);
DDbar=kron(xp,xm); DbarD=kron(xm,xp); LL=kron(yp,yp);
RR=kron(ym,ym); LR=kron(yp,ym); RL=kron(ym,yp); DR=kron(xp,ym);
RD=kron(ym,xp); DbarL=kron(xm,yp); LDbar=kron(yp,xm);
DL=kron(xp,yp); LD=kron(yp,xp); DbarR=kron(xm,ym);
RDbar=kron(ym,xm);
```

```
%%%%%%%%%%%%%%%%%%%%%%%%%%%%%%%%%%%%%%%%%%%%%%%%%%%%%%%%%%%%
%%%%% Definition of the 16 measurements  %%%%%%%%%%%%%
%%%%% Here you can choose any set of %%%%%%%%%%%%%%%%%
%%%%% 16 independent measurements  %%%%%%%%%%%%%%%%%%%
%%%%%%%%%%%%%%%%%%%%%%%%%%%%%%%%%%%%%%%%%%%%%%%%%%%%%%%%%%%%

a=zeros(4,4,16);

a(:,:,1)=HH; a(:,:,2)=HV; a(:,:,3)=VH; a(:,:,4)=VV;
a(:,:,5)=kron(F1,F2); a(:,:,6)=kron(F2,F1); a(:,:,7)=kron(F3,F3);
a(:,:,8)=kron(F4,F5); a(:,:,9)=kron(F5,F4); a(:,:,10)=kron(F6,F6);
a(:,:,11)=HD; a(:,:,12)=HL; a(:,:,13)=DH; a(:,:,14)=LH;
a(:,:,15)=LL; a(:,:,16)=RL;

%%%%%%%%%%%%%%%%%%%%%%%%%%%%%%%%%%%%%%%%%%%%%%%%%%%%%%%%%%%%
%%%%% Definition of the Gamma matrices %%%%%%%%%%%%%%%%
%%%%%%%%%%%%%%%%%%%%%%%%%%%%%%%%%%%%%%%%%%%%%%%%%%%%%%%%%%%%

base=zeros(4,4,16);

base(:,:,1)=[1 0 0 0; 0 0 0 0; 0 0 0 0; 0 0 0 0];%
base(:,:,2)=[0 0 0 0; 0 1 0 0; 0 0 0 0; 0 0 0 0 ];%
base(:,:,3)=[0 0 0 0; 0 0 0 0; 0 0 1 0; 0 0 0 0];%
base(:,:,4)=[0 0 0 0; 0 0 0 0; 0 0 0 0; 0 0 0 1];%
base(:,:,5)=1/sqrt(2)*[0 0 0 1; 0 0 0 0; 0 0 0 0; 1 0 0 0];
base(:,:,6)=1/sqrt(2)*[0 0 0 i; 0 0 0 0; 0 0 0 0; -i 0 0 0];
base(:,:,7)=1/sqrt(2)*[0 0 0 0; 0 0 1 0; 0 1 0 0; 0 0 0 0];
base(:,:,8)=1/sqrt(2)*[0 0 0 0; 0 0 i 0; 0 -i 0 0; 0 0 0 0];
base(:,:,9)=1/sqrt(2)*[0 1 0 0; 1 0 0 0; 0 0 0 0; 0 0 0 0];
base(:,:,10)=1/sqrt(2)*[0 0 1 0; 0 0 0 0; 1 0 0 0; 0 0 0 0];
base(:,:,11)=1/sqrt(2)*[0 0 0 0; 0 0 0 1; 0 0 0 0; 0 1 0 0];
base(:,:,12)=1/sqrt(2)*[0 0 0 0; 0 0 0 0; 0 0 0 1; 0 0 1 0];
base(:,:,13)=1/sqrt(2)*[0 i 0 0; -i 0 0 0; 0 0 0 0; 0 0 0 0];
base(:,:,14)=1/sqrt(2)*[0 0 i 0;  0 0 0 0; -i 0 0 0; 0 0 0 0];
base(:,:,15)=1/sqrt(2)*[0 0 0 0; 0 0 0 i; 0 0 0 0; 0 -i 0 0];
base(:,:,16)=1/sqrt(2)*[0 0 0 0; 0 0 0 0; 0 0 0 i; 0 0 -i 0];
```

```
%%%%%%%%%%%%%%%%%%%%%%%%%%%%%%%%%%%%%%%%%%%%%%%%%%%%%%%%%%%%%%%%%%%%%%%
%%%%% Definition of B matrix %%%%%%%%%%%%%%%%%%%%%%%%%%
%%%%%%%%%%%%%%%%%%%%%%%%%%%%%%%%%%%%%%%%%%%%%%%%%%%%%%%%%%%%%%%%%%%%%%%
B=zeros(16,16);

for k=1:16
    for j=1:16
        B(k,j)=trace(  a(:,:,k) * base(:,:,j)   );
    end
end

%%%%%%%%%%%%%%%%%%%%%%%%%%%%%%%%%%%%%%%%%%%%%%%%%%%%%%%%%%%%%%%%%%%%%%%
%%%%% Definition of M matrix %%%%%%%%%%%%%%%%%%%%%%%%%%
%%%%%%%%%%%%%%%%%%%%%%%%%%%%%%%%%%%%%%%%%%%%%%%%%%%%%%%%%%%%%%%%%%%%%%%

M=zeros(4,4,16); b=inv(B); b=b.*(abs(b)>1e-10);

for k=1:16
    for j=1:16
        M(:,:,k)=M(:,:,k)+b(j,k)*base(:,:,j);
    end
end
```

References

[1] Michael A. Nielsen and Isaac L. Chuang. *Quantum Computation and Quantum Information*. Cambridge University Press, 2000.

[2] Dorit Aharonov. Quantum computation. quant-ph/9812037, 1998.

[3] A. Einstein, B. Podolsky, and N. Rosen. Can quantum-mechanical description of physical reality be considered complete? *Phys. Rev.*, 47(10):777–780, May 1935.

[4] Ryszard Horodecki, Pawel Horodecki, Michal Horodecki, and Karol Horodecki. Quantum entanglement. *quant-ph/0702225*, 2007.

[5] Charles H. Bennett, Gilles Brassard, Claude Crépeau, Richard Jozsa, Asher Peres, and William K. Wootters. Teleporting an unknown quantum state via dual classical and Einstein-Podolsky-Rosen channels. *Phys. Rev. Lett.*, 70(13):1895–1899, March 1993.

[6] Asher Peres. Separability criterion for density matrices. *Phys. Rev. Lett.*, 77(8):1413–1415, Aug 1996.

[7] M. Horodecki, P. Horodecki, and R. Horodecki. Separability of mixed states: necessary and sufficient conditions. *Physics Letters A*, 223(1):1–8, November 1996.

[8] J.S. Bell. On the Einstein Podolsky Rosen paradox. *Physics 1*, page 195, 1964.

[9] John F. Clauser, Michael A. Horne, Abner Shimony, and Richard A. Holt. Proposed experiment to test local hidden-variable theories. *Phys. Rev. Lett.*, 23(15):880–884, Oct 1969.

[10] Asher Peres. *Quantum Theory: Concepts and Methods*. Kluwer, Dordrecht, 1995.

[11] Asher Peres. All the Bell inequalities. *Foundations of Physics*, 29(4):589–614, April 1999.

[12] J. E. Avron, G. Bisker, and O. Kenneth. Visualizing two qubits. *Journal of Mathematical Physics*, 48(10):102107, 2007.

[13] Charles H. Bennett, Sandu Popescu, Daniel Rohrlich, John A. Smolin, and Ashish V. Thapliyal. Exact and asymptotic measures of multipartite pure-state entanglement. *Phys. Rev. A*, 63(1):012307, Dec 2000.

[14] W. Dür, G. Vidal, and J. I. Cirac. Three qubits can be entangled in two inequivalent ways. *Phys. Rev. A*, 62(6):062314, Nov 2000.

[15] Christos H. Papadimitriou and Kenneth Steiglitz. *Combinatorial Optimization: Algorithms and Complexity*. Dover, 1998.

[16] Günther M. Ziegler. *Lectures on Polytopes*. Springer, 1995.

[17] Collins D. and Gisin N. A relevant two qubit Bell inequality inequivalent to the CHSH inequality. *Journal of Physics A: Mathematical and General*, 37:1775–1787(13), 6 February 2004.

[18] Arthur Fine. Hidden variables, joint probability, and the Bell inequalities. *Phys. Rev. Lett.*, 48(5):291–295, Feb 1982.

[19] Jon Magne Leinaas, Jan Myrheim, and Eirik Ovrum. Geometrical aspects of entanglement. *Physical Review A (Atomic, Molecular, and Optical Physics)*, 74(1):012313, 2006.

[20] Frank Verstraete, Jeroen Dehaene, and Bart De Moor. Lorentz singular-value decomposition and its applications to pure states of three qubits. *Phys. Rev. A*, 65(3):032308, Februar 2002.

[21] R. Tyrrell Rockafellar. *Convex Analysis*. Princeton University Press, 1970.

[22] Ryszard Horodecki and Michal Horodecki. Information-theoretic aspects of inseparability of mixed states. *Phys. Rev. A*, 54(3):1838–1843, September 1996.

[23] R. A. Bertlmann, H. Narnhofer, and W. Thirring. Geometric picture of entanglement and Bell inequalities. *Phys. Rev. A*, 66(3):032319, Sep 2002.

[24] K. G. H. Vollbrecht and R. F. Werner. Entanglement measures under symmetry. *Phys. Rev. A*, 64(6):062307, Nov 2001.

[25] Mary Beth Ruskai. Qubit entanglement breaking channels. *Rev. Math. Phys.*, 15:643, 2003.

[26] Chris King and Mary Beth Ruskai. Minimal entropy of states emerging from noisy quantum channels. *IEEE Trans. Info. Theory*, 47(1):192–209, Jan 2001.

[27] Mary Beth Ruskai, Stanislaw Szarek, and Elisabeth Werner. An analysis of completely-positive trace-preserving maps on 2x2 matrices. *Linear Algebra and its Applications*, 347:159, 2002.

[28] M. D. Choi. Completely positive linear maps on complex matrices. *Lin. Alg. Appl.*, 10:285–290, 1975.

[29] B. M. Terhal. Detecting quantum entanglement. *Journal of Theoretical Computer Science*, 287(1):313–335, 2002.

[30] Terhal B.M. Bell inequalities and the separability criterion. *Physics Letters A*, 271(5):319–326, July 2000.

[31] Gisin N. Hidden quantum nonlocality revealed by local filters. *Physics Letters A*, 210:151–156(6), 8 January 1996.

[32] Wu-Ki Tung. *Group theory in physics (section 10.1.4)*. World Scientific 1985 Philadelphia.

[33] J. E. Avron and O. Kenneth. in preparation.

[34] Horodecki R., Horodecki P., and Horodecki M. Violating Bell inequality by mixed spin-1/2 states: necessary and sufficient condition. *Physics Letters A*, 200:340–344(5), 1 May 1995.

[35] Reinhard F. Werner and Michael M. Wolf. Bell inequalities and entanglement. 2001, quant-ph/0107093.

[36] N. Akopian, N. H. Lindner, E. Poem, Y. Berlatzky, J. Avron, D. Gershoni, B. D. Gerardot, and P. M. Petroff. Entangled photon pairs from semiconductor quantum dots. *Physical Review Letters*, 96(13):130501, 2006.

[37] Daniel F. V. James, Paul G. Kwiat, William J. Munro, and Andrew G. White. Measurement of qubits. *Phys. Rev. A*, 64(5):052312, Oct 2001.

[38] Somshubhro Bandyopadhyay, P. Oscar Boykin, Vwani Roychowdhury, and Farrokh Vatan. A new proof for the existence of mutually unbiased bases. *Algorithmica*, 34(4):512–528, September 2007.

[39] Anna Sanpera, Rolf Tarrach, and Guifré Vidal. Local description of quantum inseparability. *Phys. Rev. A*, 58(2):826–830, Aug 1998.

[40] O. Gühne, P. Hyllus, D. Bruß, A. Ekert, M. Lewenstein, C. Macchiavello, and A. Sanpera. Detection of entanglement with few local measurements. *Phys. Rev. A*, 66(6):062305, Dec 2002.

העולם של שני קיוביטים

גילי ביסקר

העולם של שני קיוביטים

חיבור על מחקר

לשם מילוי חלקי של הדרישות לקבלת התואר מגיסטר למדעים בפיסיקה

גילי ביסקר

הוגש לסנט הטכניון - מכון טכנולוגי לישראל

כסלו תשס״ח חיפה דצמבר 2007

המחקר נעשה בהנחיית פרופ׳ יוסי אברון בפקולטה לפיסיקה.

ברצוני להביע הכרת תודה מקרב לב למנחה שלי, פרופ׳ יוסי אברון, על הדרכה יקרת ערך ותמיכה מתמדת. העידוד והעצות שלו הפכו את התיזה הזאת לאפשרית.

אני אסירת תודה לד״ר עודד קנת על עזרתו הנדיבה ועל כך שחלק את הידע והניסיון שלו בסבלנות אין קץ.

לבסוף, ברצוני להודות למשפחתי ולחבריי על התמיכה הנפשית ועל כך שהם הכוח המניע בחיי.

אני מודה לטכניון על התמיכה הכספית הנדיבה בהשתלמותי

תוכן העניינים

רשימת איורים

רשימת טבלאות

תקציר

הנושא של אינפורמציה קוונטית התפתח רבות בשני העשורים האחרונים. המאפיינים של מכאניקת הקוונטים מנוצלים עבור פיתוח אלגוריתמים חדשים ויעילים יותר בהם נעשה שימוש במצבים קוונטיים. מצב קוונטי כלשהו השייך למערכת של שני צופים יכול להיות שזור או פריק. מאז המאמר המפורסם של אינשטיין, פודולסקי ורוזן, מאמצים רבים נעשו על מנת להבין את המשמעות של שזירות במכאניקת הקוונטים. בנוסף, נעשו מאמצים ניסיוניים רבים על מנת לייצר חלקיקים שזורים בצורה יעילה ומדויקת.

מצב ρ, השייך למערכת של שני צופים, הוא פריק, אם ניתן לכתוב אותו בצורה הבאה:

$$\rho = \sum_i w_i \rho_i^A \otimes \rho_i^B$$

כאשר $\sum_i w_i = 1$ ו- $w_i > 0$.

ρ_i^A הם המצבים של תת המערכת של אליס ו- ρ_i^B הם המצבים של תת המערכת של בוב. כל מצב שאיננו פריק הוא שזור. כאשר נבצע מדידות מקומיות של מצב קוונטי שזור המחולק בין שתי מערכות, לא תמיד נוכל להסביר את הסטטיסטיקה של התוצאות המשותפות בצורה קלאסית.

השאלה האם מצב נתון ρ הוא שזור או פריק אינה שאלה קלה. אשר פרס נתן תנאי הכרחי לפריקות. לשם כך, נגדיר את הפעולה של שחלוף חלקי על מצב פריק:

$$\rho^{pt} = \sum_i w_i \rho_i^A \otimes \left(\rho_i^B\right)^T$$

ניתן לראות שאם ρ_i^B מתאר מצב של תת המערכת של בוב, גם $\left(\rho_i^B\right)^T$ מתאר מצב לגיטימי של תת המערכת של בוב ולכן ρ^{pt} כולו מתאר מצב. מטריצה המתארת מצב היא מוגדרת חיובית ולכן כל הערכים העצמיים שלה אי-שליליים. קבלנו לכן תנאי הכרחי לפריקות של מצב ρ: אם המצב ρ פריק, אז המטריצה של המצב אחרי שיחלוף חלקי ρ^{pt} מוגדרת חיובית.

הפעולה של השחלוף החלקי על מטריצה 4×4 כללית, הכתובה בבסיס החישוב, היא:

$$\begin{pmatrix} a_1 & a_2 & b_1 & b_2 \\ a_3 & a_4 & b_3 & b_4 \\ c_1 & c_2 & d_1 & d_2 \\ c_3 & c_4 & d_3 & d_4 \end{pmatrix}^{pt} = \begin{pmatrix} a_1 & a_3 & b_1 & b_3 \\ a_2 & a_4 & b_2 & b_4 \\ c_1 & c_3 & d_1 & d_3 \\ c_2 & c_4 & d_2 & d_4 \end{pmatrix}$$

בעזרת הגדרה זו נוכל לבדוק את התנאי על כל מטריצה 4×4 שמתארת מצב.

התנאי ההכרחי לפריקות של אשר פרס הוא גם מספיק עבור מערכות של שני קיוביטים או מערכות של קיוביט וקיוטריט. עובדה זו הוכחה על ידי בני משפחת הורודצקי בעזרת "עדי שזירות" והקשר בינם לבין העתקות חיוביות על מרחבי הילברט.

משפט: מצב ρ הוא שזור אם ורק אם קיים אופרטור W, כך ש- $Tr(W\sigma) \geq 0$ עבור כל מצב פריק σ ו- $Tr(W\rho) < 0$. האופרטור W נקרא עד שזירות.

מבחן נוסף לשזירות הוא אי שוויון בל. זהו מבחן מספיק אך לא הכרחי, כלומר, קיימים מצבים שזורים שלא מפרים אף אי שוויון בל, אך אם מצב כלשהו מפר אי שוויון בל הוא שזור. התיאוריה של בל מדברת על קיום של משתנים חבויים מקומיים. בל הראה שלא ניתן ליישם את התיאוריה הזו למכאניקת הקוונטים. אם מניחים קיום של משתנים מקומיים חבויים, הסטטיסטיקה של תוצאות מדידות מקומיות שנעשו על ידי אליס ובוב צריכה לקיים קבוצה של אי שוויונות. אלו הם אי שוויונות בל. מכיוון שקיימים מצבים שזורים שעבורם אי שוויון בל מופר, ניתן להסיק שלא ניתן לתאר אותם במסגרת תורה שמכילה משתנים מקומיים חבויים.

אי שוויון בל חשוב הוא אי שוויון CHSH. במקרה זה ישנם שני צופים, אליס ובוב, כאשר לכל צופה יש שתי מדידות אפשריות ולכל מדידה יש שתי תוצאות אפשריות. למשל, אליס יכולה למדוד ספין בכיוון $\hat{a}$ או $\hat{a}'$ ובוב יכול למדוד ספין בכיוון $\hat{b}$ או $\hat{b}'$. אופרטור בל במקרה זה יהיה:

$$B = \hat{a}\cdot\vec{\sigma}\otimes\left(\hat{b}+\hat{b}'\right)\cdot\vec{\sigma} + \hat{a}'\cdot\vec{\sigma}\otimes\left(\hat{b}-\hat{b}'\right)\cdot\vec{\sigma}$$

אי שוויון בל הוא $-2 \le \langle B \rangle \le 2$.

אי שוויונות בל כלליים יותר ניתן לקבל על ידי הגדלת מספר הצופים, הניסויים או מספר התוצאות האפשריות עבור כל ניסוי.

ישנה דרך כללית לקבלת אי שוויונות בל עבור מספר כלשהו של צופים, מספר כלשהו של ניסויים אפשריים לכל צופה ומספר כלשהו של תוצאות אפשריות לכל ניסוי. אשר פרס הציע לבנות את אי שוויונות בל בעזרת וקטורי פרקש. כל אי שוויון בל ניתן לרשום בצורה:

$$\sum F^K P_K \ge 0$$

כאשר P_K הם הסתברויות של מדידות וניתן למצוא אותם בניסיון והמקדמים F^K הם שלמים. הווקטור F^K נקרא וקטור פרקש. בעבודה זו, אנו נסכם את התוצאות העיקריות של אשר פרס בנושא זה ונשתמש בהן על מנת לבנות את אי שוויון CHSH.

עולם המצבים, העדים ואי שוויונות בל עבור שני קיוביטים ניתן להצגה גיאומטרית בשלושה מימדים. עולם זה מיוצג על ידי מטריצות הרמיטיות 4×4, כלומר הוא בעל 16 מימדים ולכן עלינו להשתמש ביחס שקילות מתאים על מנת להוריד את מספר המימדים מ- 16 ל- 3. השימוש במחלקות השקילות של פעולות מקומיות סטוכסטיות ותקשורת קלאסית (SLOCC) הוא נפוץ עבור מצבים ובעבודה זו נראה שניתן לכלול גם את עדי השזירות ואי שוויונות בל בתיאור. התיאור הגיאומטרי נשאר נאמן לדואליות בין מצבים פריקים לבין עדי שזירות ומאפשר לתת הוכחות פשוטות ואלגנטיות לתוצאות מסובכות.

במסגרת יחס השקילות של פעולות מקומיות סטוכסטיות ותקשורת קלאסית אנו רוצים לשים באותה מחלקת שקילות כל שני מצבים, כך שמהמצב הראשון ניתן לקבל את המצב השני בהסתברות גדולה מאפס, על ידי פעולות לוקאליות של אליס ובוב. מכיוון שיחס שקילות הוא יחס סימטרי, נאפשר לאליס ובוב לבצע פעולות הפיכות בלבד. דרך מתמטית לתאר את מחלקת השקילות של מצב ρ כלשהו היא:

$$\rho \sim \rho^M = M\rho M^\dagger \qquad M = A\otimes B \qquad A,B \in SL(2,\mathbb{C})$$

התיאור בשלושה מימדים מאפשר לנו לתת הוכחה גיאומטרית שעבור שני קיוביטים, המבחן של פרס לשזירות הוא "אם ורק אם". בנוסף, אנו מראים שאי שוויון בל CHSH יכול להיות מתואר על ידי מעגלים בתמונה התלת ממדית. במקרה של CHSH, לאליס ולבוב יש בחירה מתוך שני ניסויים לכל אחד ולכל ניסוי יש שתי תוצאות אפשריות. תיאור זה של אי שוויון CHSH מאפשר לפתור גיאומטרית את בעיית האופטימיזציה של ההפרה המקסימאלית של אי השוויון. לכל מצב נתון בתמונה ניתן למצוא בקלות את עד השזירות שמתאים לאי שוויון CHSH עבורו נקבל את ההפרה המקסימאלית, אם בכלל תתכן הפרה. לבסוף, בעזרת חישוב נומרי, נראה שאם מאפשרים לאליס ולבוב לבחור מתוך שלושה ניסויים במקום שניים, איננו מגלים מחלקות שקילות נוספות של מצבים שזורים מעבר למחלקות שגילינו במקרה של CHSH.

לרעיון של עדי שזירות יש משמעות מעשית. אם נרצה להוכיח בצורה ניסויית את הקיום של שזירות, נוכל להשתמש בשתי גישות שונות. האחת היא למצוא את המצב כולו ולהשתמש במבחן פרס לשזירות שהזכרנו כאן. השנייה היא למדוד את ערך התצפית של עד שזירות מתאים. השיטה השנייה היא יותר חסכונית מכיוון שמספר המדידות הדרוש קטן יותר, בעוד שלשיטה הראשונה נדרשות לא פחות מ- 16 מדידות. אנו מציגים קבוצה של מדידות שכל אחת מהן היא מכפלה של הטלות. הקבוצה הזו היא אופטימאלית להוכחת שזירות מבחינת מספר המדידות הנדרש.

אנו מתייחסים לשתי אפשרויות שונות. בראשונה, אנו מאפשרים למדוד קבוצת מדידות מצומצמת שמורכבת מהמדידות הסטנדרטיות בלבד $\left\{\left|H\right\rangle,\left|V\right\rangle,\left|D\right\rangle,\left|\bar{D}\right\rangle,\left|L\right\rangle,\left|R\right\rangle\right\}$, כאשר:

$$\left|H\right\rangle=\left|0\right\rangle$$
$$\left|V\right\rangle=\left|1\right\rangle$$
$$\left|D\right\rangle=\tfrac{1}{\sqrt{2}}\left(\left|0\right\rangle+\left|1\right\rangle\right)$$
$$\left|\bar{D}\right\rangle=\tfrac{1}{\sqrt{2}}\left(\left|0\right\rangle-\left|1\right\rangle\right)$$
$$\left|L\right\rangle=\tfrac{1}{\sqrt{2}}\left(\left|0\right\rangle+i\left|1\right\rangle\right)$$
$$\left|R\right\rangle=\tfrac{1}{\sqrt{2}}\left(\left|0\right\rangle-i\left|1\right\rangle\right)$$

באפשרות השנייה, אנו מניחים שכל מדידה היא אפשרית. אנו מרשים למדוד את מצבי הקיטוב הבסיסיים $\left|H\right\rangle$ ו- $\left|V\right\rangle$ ובנוסף כל קומבינציה שלהם בעלת הצורה $\tfrac{1}{\sqrt{2}}\left(\left|H\right\rangle+e^{i\theta}\left|V\right\rangle\right)$.
בכל מקרה, אם לא נבצע 16 המדידות בלתי תלויות, לא נוכל לשחזר את המצב במלואו, אלא נוכל להגיד רק אם קיימת שזירות.